Mid-Devonian sinistral transpressional movements on the Great Glen Fault: the rise of the Rosemarkie Inlier and the Acadian Event in Scotland.

J.R. Mendum[1] *& S.R. Noble*[2]

[1]British Geological Survey, Murchison House, West Mains Road, Edinburgh, EH9 3LA

[2]NERC Isotope Geosciences Laboratory, British Geological Survey, Kingsley Dunham Centre, Keyworth, Nottingham, NG12 5GG

e-mail: jrme@bgs.ac.uk

Abstract

The Rosemarkie Inlier is a small fault-bounded lens of interleaved Moine psammites and possible Lewisianoid orthogneisses with distinctive leucogranite veins and pods that lies adjacent to the Great Glen Fault (GGF). The basement rocks and most of the leucogranites are strongly deformed and tightly folded with foliations generally steeply dipping and a locally well-developed NE-plunging rodding lineation. Mid-Devonian sandstone and conglomerate unconformably overlie the inlier on its western side. Monazite from a deformed leucogranite vein gave a mean ID-TIMS $^{207}Pb/^{235}U$ age of 397.6 ± 2.2 Ma and acicular zircons gave a compatible concordant ID-TIMS U-Pb age of 400.8 ± 2.6 Ma, dating emplacement as mid-Devonian. Xenocrystic zircons from the leucogranites and complex zoned zircons from two adjacent tonalitic gneisses gave LA-MC-ICP-MS concordant ages between 2720 and 2930 Ma confirming their Archaean Lewisianoid origin. Leucogranite emplacement is interpreted to mark the onset of Acadian transpression and sinistral strike-slip movement on the GGF that resulted in multi-phase deformation and oblique exhumation of the Rosemarkie Inlier. The sequence and structure of the Early Devonian Meall Fuar-mhonaidh Outlier, 32 km farther SW along the GGF, are also linked to this tectonic event, which was apparently localised along the main terrane-bounding faults in Scotland.

End of Abstract

The Great Glen Fault (GGF) is a major geological and topographical feature that transects the Highlands of Scotland, separating the Grampian Highlands to the southeast from the Northern Highlands to the northwest. The fault passes offshore into the Moray Firth (Fig. 1), where it forms a major sub-vertical structure (Andrews *et al*. 1990). The fault can be traced for a further 23 kilometres northeast into the West Moray Firth Basin into deformed Mesozoic strata (Bird *et al*. 1987; Underhill 1991). The full role of the GGF in the geological history and tectonic development of the Scottish Highlands remains unclear, but it appears to have acted as a Neoproterozoic basin-bounding fault (Banks & Winchester 2004) and has undoubtedly been the focus of significant sinistral movements during the Palaeozoic (Johnstone & Mykura, 1989; Stewart *et al*. 1999). Minor sinistral, dextral and vertical movements followed in Mesozoic and Cenozoic times (Rogers *et al*. 1989; Andrews *et al*. 1990; Underhill & Brodie, 1993; Roberts & Holdsworth, 1999). Exposure along the Great Glen is generally poor, but farther SW, mylonites and blastomylonites attest to ductile shearing at mid-crustal levels (9-16 km) with later cataclasite, phyllonite and breccia development reflecting shallower level brittle movements (Stewart *et al*. 1999).

The Rosemarkie and Cromarty inliers crop out adjacent to the GGF surrounded by Devonian rocks (Fig. 1). The Rosemarkie Inlier, some 2 km wide and 9 km long, lies on the Black Isle adjacent to the GGF whose trace runs up to 500 m offshore (Fig. 2). It exposes deformed amphibolite-facies psammites, subsidiary semipelites, amphibolitic mafic bodies and laminated felsic and mafic gneisses, all cut by abundant, typically salmon pink, leucogranite veins and sheets (Rathbone & Harris 1980; Fletcher *et al*. 1996). Exposure is effectively limited to coastal outcrops (Fig. 3a), with a few weathered inland outcrops. To the SW and NE the inlier is fault-bounded, but on its NW side mid-Devonian sandstones and conglomerates unconformably onlap the inlier. Palynological data from this Orcadian sequence show that its basal beds were deposited in the late Eifelian at c. 393 Ma (Marshall *et al*. 2007). The main psammitic and gneissose lithologies are similar to those of the Neoproterozoic Moine succession and Archaean Lewisianoid inliers of the Northern Highlands respectively, but they differ considerably

from the nearest Moine rocks, Loch Eil Group psammites that crop out some 20 km to the NW.

The rocks of the inlier are widely altered, fractured and crushed with breccia and gouge developed. The exception to this is a section below Learnie Farm between [NH 760 712] and [NH 767 620] where brittle deformation was limited and earlier ductile deformation structures are seen clearly. Here, Rathbone & Harris (1980) recognised four discrete phases of ductile deformation with the leucogranites deformed by the latter three phases. The majority of the leucogranite veins show clear evidence of intrusion at an early stage of the main deformation (D_2) (Rathbone & Harris 1980). The deformation phases in the inlier have been correlated with those of the Moine rocks and hence the leucogranites were thought to be of Ordovician age or older (Rathbone 1980).

The inlier was exhumed after emplacement of the leucogranite veins but prior to deposition of the adjacent late Eifelian to Givetian sequence. To provide a lower age constraint on deformation and exhumation, samples of leucogranites were collected for U-Pb isotopic dating. Samples of the adjacent gneisses were also taken to ascertain their relationship with the Lewisianoid gneisses that underlie the Moine Supergroup of the Northern Highlands. Stratigraphical units and related ages quoted in this paper are based on the current International Commission on Stratigraphy chart that largely follows Gradstein *et al*. (2004).

Tectonic Setting

Studies of the later stages of the Caledonian Orogeny in the Northern Highlands have focused on the formation of the Moine Thrust Zone at its western margin, and on the uplift and intrusion history of its interior and its southeast side. The Moine Thrust Zone was active mainly during the Scandian event between c. 437 Ma and c. 430 Ma (Johnson *et al*. 1985; Dallmeyer *et al*. 2001; Goodenough *et al*. 2006) with later extensional movements continuing spasmodically to 408 Ma (Freeman *et al*. 1998). Dewey & Strachan (2003) argued that Scandian deformation is absent from the Grampian Highlands to the SE of the GGF, and hence postulated that at least 700 km of sinistral movement took place along the GGF between 425 Ma and 395 Ma. The waning phases of the Caledonian Orogeny in the Northern Highlands were marked by intrusion of

93 granitoid plutons coeval with regional uplift and significant lateral movements on the
94 main NE-trending faults (Watson 1984). Documented examples include the Clunes
95 Tonalite (428 ± 2 Ma; Stewart *et al*. 2001) and the Strontian Pluton (425 ± 3 Ma; Rogers
96 & Dunning, 1991), both linked to movements on the GGF (Hutton 1988), and the
97 Ratagain Pluton (425 ± 3 Ma; Rogers & Dunning 1991), linked to movements on the
98 Strathconon Fault (Hutton & McErlean 1991).
99
100 The main development of the Acadian Orogeny lies in eastern North America where
101 Avalonia collided with Laurentia; the resultant deformation, metamorphism and related
102 igneous intrusion events lasted from 420 – 395 Ma (Van Staal *et al*. 1998; Van Staal &
103 Whalen 2006; Zagorevski *et al*. 2007). In the British Isles the Acadian event resulted
104 from early collision of an Armorican microcontinent with the Avalonian part of
105 Laurussia at the northwest margin of the Rheic Ocean. The collision caused the Midland
106 platform (microcraton) to indent the Welsh Basin and Late Palaeozoic basins of central
107 and northern England (Woodcock *et al*. 2007). Acadian deformation and related
108 metamorphism occurred in the Lake District, Wales, and southern Britain between 400
109 and 390 Ma (Soper & Woodcock 2003; Sherlock *et al*. 2003). Acadian volcanic rocks
110 seem to be absent from the British Isles and 'Acadian' granites are restricted to the
111 Southern Uplands and the Lake District. The nature of the Acadian event in Scotland is
112 equivocal, although structures in the Midland Valley, e.g. the Strathmore Syncline, have
113 been attributed to mid-Devonian (c. 400 Ma) sinistral transpression (Soper *et al*. 1992;
114 Jones *et al*. 1997).
115
116 In Baltica the Acadian event is absent and there is only evidence of an extended
117 history of Devonian uplift and exhumation of the Western Gneiss region of Norway
118 (Krabbendam & Dewey, 1998; Johnston *et al*. 2007; Walsh *et al*. 2007) and formation of
119 large sinistral transtensional basins (Osmundsen & Andersen, 2001; Eide *et al*. 2005).
120 Uplift and extension here lasted from at least 410 Ma through to 370 Ma.
121
122 **The lithology and structure of the Rosemarkie Inlier**

Hugh Miller (in 1885) and John Horne (in 1890) mapped the Rosemarkie Inlier during the primary geological survey and brief descriptions of the lithologies and petrography are given in the Geological Survey of Scotland Memoir for the area (Horne, 1923). Horne noted the distinctive character of the rocks and the abundance of alkali-felspar-rich granitic material. He commented on their similarities to the Moine psammites, but also speculated that the hornblendic felsic gneisses may equate to the 'Lewisian floor' to the Moine succession (i.e. the Lewisianoid gneisses). He even suggested (p. 58) that the rocks may be a 'distinct group of Moine rocks brought up by the Great Glen Fault'. Subsequently, P. A. Rathbone carried out detailed work on the inlier as part of his Ph.D. (Rathbone 1980; Rathbone & Harris 1980) and A. J. Highton remapped the southern part of the Rosemarkie Inlier and questioned the nature of the protolith of the felsic and mafic gneisses (Fletcher *et al*. 1996). Much of the structural data used here has been abstracted from Rathbone (1980).

Lithology

The Rosemarkie Inlier consists of grey, flaggy, typically thinly banded siliceous to micaceous psammites with subsidiary semipelites and pelites. Thin quartzofeldspathic lenticles impart a weakly gneissose appearance to the rocks. The psammites are interleaved with laminated to thinly banded felsic and mafic gneisses on scales varying from a few centimetres to ten of metres. The felsic gneisses consist essentially of quartz-plagioclase-biotite with variable hornblende content and are interlaminated with abundant amphibolitic mafic gneisses. Thicker amphibolitic mafic units and hornblendic ultramafic lenses, locally with agmatitic net-veins, also occur within these gneisses, features characteristic of the basement Lewisianoid inliers within the Moine succession. No obvious shear zones or dislocations can be identified at psammite-gneiss contacts and in places the distinction is quite cryptic. Discrete mafic amphibolite sheets and lenses are also common in the psammites, semipelites and the gneisses. These lithologies all contain a strong layer parallel fabric that is folded by F_2, F_3 and F_4 folds. The rocks show evidence of pervasive recrystallisation with quartz, feldspar, hornblende, biotite and muscovite defining a composite S_1-S_2 fabric. The metamorphic assemblages are characteristic of lower amphibolite facies metamorphism although index minerals are

largely absent and retrogression effects are widespread. Elongate garnet porphyroblasts are developed in the pelitic units and deformed by the D_2 crenulation fabric, whereas the abundant small muscovite and shimmer aggregate porphyroblasts overprint the main S_2 foliation (Fletcher *et al.*1996).

Pink to red, foliated and lineated leucogranite sheets, lenses and veins are diagnostic of the Rosemarkie Inlier. The intrusions are typically 0.3 to 1 m wide but range from a millimetre up to 5 m in thickness. They are generally parallel sided and show sharp planar contacts with the country rocks (Fig. 3a), but some very thin veins do show diffuse margins. Although strongly deformed, the leucogranite veins are clearly discordant to the host banding in numerous instances (Rathbone & Harris, 1980). Typically, the angle of discordance is <5° but locally high angles are seen. The granite is variable from fine-grained to coarse-grained and partly pegmatitic; in parts it contains pink potash feldspars, typically augened. Its mineralogy is essentially quartz, potash feldspar and plagioclase, with minor muscovite and biotite and accessory zircon, magnetite or ilmenite, and rare apatite, monazite and titanite. Secondary chlorite (after biotite), zoisite, carbonate and rarely sodic amphibole are developed (Fletcher *et al.* 1996). In some areas white muscovite-bearing leucogranite sheets and veins intrude the Moine psammites and semipelites; they show similar features to the pink veins. Although many of the leucogranite veins show evidence of strong deformation, others show deformation features, lower strains and mineralogies indicative of lower temperature and brittle shearing, suggesting they were emplaced at higher crustal levels.

Structure

Rathbone & Harris (1980) recognised four deformation phases in the Rosemarkie Inlier. The planar fabrics parallel to the compositional banding and fine-scale interleaving of Moine psammites and Lewisianoid gneisses were attributed to the D_1 event. Tight to isoclinal minor folds are moderately abundant and are attributed to D_2. A related planar schistosity (S_2) and associated lineation (L_2) are pervasively developed. F_3 open to tight folds demonstrably refold the F_2 folds and S_2 fabrics and are abundant on a small- and medium-scale. Their axes normally plunge moderately to the NE and verge

towards the SE. However, Rathbone & Harris (1980) noted that F_3 fold hinges are commonly curvilinear through up to 120°. Their axial planes are typically upright with an S_3 schistosity widely developed. D_4 folds control much of the variation in strike and dip. They also plunge towards the northeast but their vergence is towards the northwest. Their axial planes are generally upright, and only rarely is an associated cleavage developed. F_4-F_3 and F_3-F_2 fold interference patterns are seen in the psammite-semipelite lithologies and in the felsic and mafic gneisses. At [NH 765 615] interleaved Moine and Lewisianoid rocks are folded by a very tight metre-scale fold (F_2) that is in turn refolded by a D_3 synform. The leucogranite veins contain a strong L-S fabric defined by strongly attenuated quartz and feldspar with minor thin stringers of biotite and sparse muscovite development. The lineation and foliation is contiguous with L_2 and S_2 in the adjacent Moine and Lewisianoid rocks where it is defined by quartz, feldspar and in the mafic rocks, hornblende alignment. L_2 in the leucogranite is a millimetre-scale rodding of quartz and pink feldspar; it locally dominates to give an L-tectonite. In places there are spectacular F_2-F_3 interference folds involving the leucogranite veins (Fig. 3b). Rathbone & Harris (1980, Figure 4) documented examples of fold interference patterns involving the leucogranite veins and also showed that the prominent quartz lineation (L_2) was locally modified by later D_3 structures.

Fenitization, carbonate veining, brecciation and minor faulting dominate the southern exposures in the Rosemarkie Inlier, but on the coastal section below Learnie Farm later brittle deformation effects are minimal. Here, the banding/foliation strikes mainly between northeast and north, dips range from vertical to moderately eastwards, and L_2 plunges northeast at moderate angles (37° to 050°) (Fig. 4). L_2 is co-linear with the majority of the F_2 and F_3 axes, as indicated by the distribution of poles to foliation/bedding.

Leucogranite Textures

In thin section the foliated and lineated leucogranites from Learnie Shore are dominated by quartz and feldspar ‘ribbons’, the latter being lenticular, typically measuring 8 to 12 mm long and 0.3 mm to 1 mm wide in the S-L plane. The potash and plagioclase feldspars are disaggregated and fragmented with some sericitisation and new

quartz growth. In the quartz ribbons grain-size reduction has occurred giving rise to recrystallized aggregates 0.03 mm to 0.6 mm across, that exhibit tessellate grain boundaries, strain shadows, fine inclusion trails and extensive sub-grain development. Small ragged' biotites, in part altered to chlorite, in parts form discontinuous trails marginal to the feldspar laminae. Ilmenite or magnetite form irregular altered aggregates and may have released iron to give the prominent pink to red feldspar colouring. The 'ribbons' have formed in response to the strong deformation with the elongate feldspars now effectively being porphyroclasts. Thin sections normal to the lineation show potash feldspar and plagioclase porphyroclasts commonly 3 to 4 mm across. They show strain twinning, embayed margins and locally marginal myrmekite development. The typical porphyroclast size and dimensions of the ribbons suggest that the leucogranite was originally a medium- or even coarse-grained granite. The petrographic features in the leucogranites are compatible with strong deformation under lower amphibolite-facies conditions. As the lineation clearly defines the stretching direction (Ls), Rathbone (1980) measured the shapes of the quartz aggregates in the deformed leucogranite using them to define the principal planes of the strain ellipsoid. Taking the quartz as initially equant, a common circumstance in granites, he obtained X:Y:Z values of 18:2.5:1. This strain is prolate with a *k* value of 2.88 (Flinn 1962).

In parts the leucogranite shows an augen texture with potash feldspars up to 1 cm across. Some appear to reflect relic feldspar crystals but other have grown during deformation and recrystallization. Although some augen show δ and σ tails that imply a shear sense, many have a neutral geometry. M Stewart (*pers. com*. 2004) noted that the shear sense was generally consistent within individual intrusions and in the pink leucogranite sheets was generally sinistral. In contrast the white muscovite-bearing sheets generally had internal and marginal fabrics implying a dextral shear sense. Stewart also recorded that there was evidence of later more brittle dextral shearing, generally focused at the margins of the leucogranite veins and in the more pelitic units. This deformation was accompanied by extensive chlorite growth.

Cromarty Inlier

The Cromarty Inlier, measuring c. 9 km x 2.7 km, lies immediately northeast of the Rosemarkie Inlier, nestling against the GGF (Fig. 1), and is similarly onlapped by the late Eifelian sandstones and conglomerates. The inlier exposes variably siliceous to micaceous psammites with subsidiary semipelites, cut by garnet amphibolite bodies: the metasedimentary lithologies have been assigned to the Moine Supergroup (Rathbone & Harris 1980). The pelitic units are garnetiferous and contain quartzofeldspathic segregations and white-mica aggregates with sparse relict fibrolite and more rarely ragged, strained kyanite blades (Rathbone & Harris 1980). Thin quartzofeldspathic veins and porphyroblasts and segregations of pink feldspar are common and there is evidence of *in situ* mobilisation of the psammites and semipelites. Several dyke-like masses of red pegmatitic granite of unknown age, some over 6 metre thick, cross cut the mafic and metasedimentary rocks.

The structures in the Cromarty Inlier correlate in part with those in the Rosemarkie Inlier. Rathbone & Harris (1980) reported that a single early planar fabric (S_1-S_2?) is folded by the dominant F_3 folds. In the southern part of the inlier F_3 axial planes are sub-vertical and first trend NE-SW but swing to E-W and then SE-NW at South Sutor stacks (Fig.2). F_3 axes similarly plunge gently NE and also swing to plunge moderately NW. In the northern part of the inlier F_3 axial traces trend SE-NW and axial planes dip NE at c. 60°. F_3 axes plunge gently to moderately both NW and SE. The folds have no consistent vergence and as in the Rosemarkie Inlier, the F_3 axes are curvilinear. F_4 folds are developed on several scales; their axes plunge consistently NE and they have steeply dipping axial planes.

Devonian Rocks

At the southwest end of the Rosemarkie Inlier is a thin, wedge-shaped and fault-bounded sliver of early Devonian Lower Old Red Sandstone (ORS) rocks that is overlapped to the west by mid-Devonian conglomerate (Fig. 2). The succession, termed the Den Siltstone Formation by Fletcher *et al*. (1996), consists of indurated breccio-conglomerates and chocolate brown to green-grey siltstones and silty sandstones. Lithologically, they are similar to Struie Group that crops out farther northwest (Trewin & Thirlwall 2002). The rocks dip moderately to very steeply westwards, but are affected

by small-scale faulting with gouge commonly developed and sub-horizontal slickensides locally present. The bounding faults to this Lower ORS sequence extend into the overlying mid-Devonian succession.

The Meall Fuar-mhonaidh Outlier

The Meall Fuar-mhonaidh Outlier exposes a c. 2 kilometre-thick sequence of Lower ORS sandstones and conglomerates and minor siltstones and mudstones (Fig. 5) (Mykura & Owens 1983). The fault-bounded outlier measures 15 km long and c. 3 km wide and lies adjacent to the GGF and Loch Ness, some 32 kilometres SW of the Rosemarkie Inlier (Fig.1). Mykura & Owens (1983) collected a siltstone sample from the Drumbuie Burn by Drumnadrochit for palynological studies. This yielded fragmentary plant material and miospores indicating a late Emsian or early Eifelian age. The dominant lithology is a red-brown to purple, micaceous sandstone with thin mudstone partings and minor siltstone and conglomerate interbeds. Thick units of pink to red-brown, arkosic, gritty, coarse-gained sandstone occur in the southern part of the outlier and around Urquhart Castle (Fig. 5). Prominent lenticular units of poorly sorted and unbedded conglomerate and breccio-conglomerate, 50m to 400m thick, interdigitate with the sandstones. Moine psammites form most of the conglomerate clasts with subordinate semipelite, vein quartz, granite-gneiss, microgranite and some locally derived sandstone. Conglomerate-sandstone contacts are generally sharp and planar, but at [NN 4620 2215] a large ‘flame’ structure is developed; a 3-4m wide septum of steeply dipping silty sandstone penetrates the overlying conglomerate for some 50 metres.

At the northeast end of the outlier near the top of the succession lies the Creag Nay Conglomerate, a highly lensoid, clast-supported, breccio-conglomerate unit, bounded on its eastern side by a steep fault. It consists of large angular clasts of psammite and pink to orange leucogranite in a coarse-grained sandstone matrix. Mykura & Owens (1983) interpreted the unit as the product of a proximal debris flow derived from the east.

The Meall Fuar-mhonaidh sequence is folded into a broad syncline with minor folds and steeper dips developed in the southeast part of the outlier closer to the GGF (Fig. 4).

Minor fold axes typically plunge gently to the E and NE or to the W and SW. Cross-section restorations show that overall shortening across the outlier totals some 25%. At the southern end of the outlier Mykura & Owens (1983) recorded that the Devonian rocks have been thrust and faulted against brecciated and cataclastic Moine psammites. At NH 449 188 shattered pebbly sandstones are separated from the underlying Moine psammites by a mylonite zone that dips c. 25° SE. Mykura & Owens (1983) also postulate a thrust at the Devonian-Moine boundary immediately north of Loch a'Bhealaich to explain its sinuous nature and the steep dips in the overlying conglomerates and sandstones. The northwestern boundary of the outlier is unexposed but its overall orientation suggests that it is a steeply dipping NE-trending fault. Faults in the outlier generally trend north and NE and postdate the folding and thrusting.

The succession preserved in the Meall Fuar-mhonaidh Outlier represents a fluviatile and lacustrine sequence, rapidly deposited in late Emsian times in a restricted rift basin with marginal alluvial fans (Mykura & Owens 1983). Contractional deformation linked to movements along the GGF may have overlapped the later stages of sedimentation, and subsequently generated folding, localised thrusting, and faulting in the outlier. The structural pattern is compatible with a positive flower structure linked to sinistral transpression along the GGF.

Geochronology

Previous studies

Rathbone (1980) reported strongly discordant zircon U-Pb data defining a chord with a lower intercept at 384 Ma from a leucogranite vein below Learnie [NH 766 618]. The bulk zircon fractions were analysed by R.A. Cliff at Leeds University and consisted of old grains, neocrystalline grains, and composite grain cores and rims. The data were obtained when zircons were not processed to reduce the effects of lead loss, and hence this age likely underestimated the true age of new zircon growth. The leucogranites were interpreted as deformed by a D_2 event that was correlated directly with the deformation sequence seen in the Moine succession. Hence, as the rocks were altered and lay adjacent

to the GGF the lower intercept age was discounted as due to subsequent leaching and consequent lead loss.

Sampling and analytical techniques

For this study four samples of leucogranite and two of adjacent thinly banded hornblendic felsic gneisses were collected from the shore section below Learnie Farm (Figure 3a). Zircon and monazite were recovered from the c. 3 kg samples using standard crushing, heavy liquid and isodynamic magnetic separation techniques. Zircons from two leucogranite samples were not analysed as the grains proved insufficiently robust to survive either air or chemical abrasion due to abundant cracks and probable high U contents. Sample location grid references are given in Tables 1 and 2.

Mineral grains selected for TIMS analysis and zircons for LA-MC-ICP-MS analysis were hand-picked under ethanol and only the highest quality crack-free grains were chosen. Cathodoluminescence images of the main types of zircon grains in the leucogranite and gneisses are shown in Fig. 6. Zircons selected for TIMS analysis were abraded following Krogh (1982) to reduce Pb loss. All minerals selected for TIMS analysis were washed in distilled 2N HNO_3 at c. 60° C and ultra-pure water, spiked with a $^{205}Pb/^{235}U$ tracer and dissolved in ultra-pure acids, and processed through chemistry following Krogh (1973) with modifications as described by Corfu & Noble (1992). Data were mainly obtained on a VG 354 mass spectrometer fitted with an ion-counting Daly detector, with some data obtained on a Triton mass spectrometer using an ion-counting secondary electron multiplier. Procedural blanks were <10 pg and <0.1 pg for Pb and U, respectively. Raw data were reduced using PbDat (Ludwig 1993). The common Pb isotope composition used in data reduction was estimated using the two-stage model of Stacey & Kramers (1975).

Zircons from the samples GX 1732 and 1737 were selected for analysis by LA-MC-ICP-MS and subjected to chemical abrasion (CA) following Mattinson (2005), as this has been shown to improve concordance of the ablated minerals (M. Horstwood. pers. comm. 2006). The grains were annealed at 900 °C for 60 hrs and then leached at 180 ° C in 29M

370 HF for 10 hrs to remove domains that could contribute to Pb loss. Zircons from sample
371 GX1732 were not significantly affected; whereas some GX1737 grains were reduced in
372 volume by up to c. 30% (see Fig. 6 e). The zircons were then mounted in 25 mm
373 diameter epoxy resin discs and polished to remove c. 40% of the grain thicknesses to
374 yield cross sections. Grains were imaged in backscatter electron (BSE) and
375 cathodoluminescence (CL) modes using a scanning electron microscope (SEM) to
376 examine the zircon internal zonation, thus allowing selection of appropriate areas for
377 laser ablation analysis. Data were obtained on a Nu HR MC-ICP-MS using analytical
378 protocols based on Horstwood *et al*. (2003). Raw data were reduced using an in-house
379 Excel spreadsheet. TIMS and MC-ICP-MS reduced data were plotted using Isoplot
380 (Ludwig 2003). Sample information and U-Pb data are summarized in Tables 1 and 2,
381 and plotted on Figure 7. TIMS errors in the data tables and plotted on concordia
382 diagrams are quoted at the 2σ level.
383
384 *Results*
385 Two distinctive zircon morphologies were recognised in the leucogranites. Stubby,
386 internally complex-zoned, faceted to rounded, partly resorbed zircons were the most
387 abundant type, but well-faceted, acicular zircons were also present (see Fig. 6). Titanite
388 was the principal secondary U-bearing accessory phase in the leucogranites, except in
389 GX 1734 where monazite was present.
390
391 The acicular zircons typically have large aspect ratios, up to 10:1, and show strong
392 oscillatory compositional zoning, visible both under the binocular microscope and by CL
393 (Fig. 6a). Cores occur in all but the smallest acicular grains. U contents in the acicular
394 zircons are relatively high (c. 700 ppm, Table 1) with the highest U-zones (grey low CL
395 areas - Fig. 6a) occurring at the grain tips. Multi-grain fractions of acicular zircons from
396 sample GX 1731 were selected for analysis by TIMS to constrain the emplacement age
397 of the leucogranites. Each fraction comprised abraded small grains, <50 μm long,
398 exhibiting only simple oscillatory zoning. Given their small size and delicate elongate
399 form, the grains were only lightly abraded, making total elimination of Pb-loss difficult.
400 Additional analyses using CA-TIMS were not pursued as the high-U domains that best

represent new zircon growth during leucogranite emplacement and crystallization would have been removed during the preliminary leaching steps.

Monazite was found only in leucogranite sample, GX 1734, where it forms sharply faceted greenish-yellow euhedral crystals and crystal fragments up to 100 μm long. Fe-oxide inclusions are common in most of the monazite grains but only inclusion-free crystals were selected for analysis. This high quality monazite is considered to be the most reliable and preferred mineral for dating the leucogranite crystallization at Rosemarkie. Although zircon is abundant in the leucogranites, its near ubiquitous inheritance is a serious impediment to achieving concordant TIMS ages. A similar problem has previously been noted in Himalayan leucogranites (e.g. Noble & Searle 1995).

One acicular zircon fraction from sample GX 1731 is reversely discordant but overlaps the concordia curve, yielding a concordia age (Ludwig 2003) of 400.8 ± 2.6 Ma (Fig. 7a). The second zircon fraction is normally discordant and slightly younger than 400 Ma. Its position on the concordia plot is consistent with Pb-loss coupled with a small amount of inherited older zircon present.

The monazite data are slightly reversely discordant, which results from excess ^{206}Pb, as is normally found in pristine monazite that does not show Pb-loss (Schärer 1984). The data spread along concordia but all four analyses overlap within error. The crystallization age is best constrained by the average monazite $^{207}Pb/^{235}U$ age of 397.6 ± 2.2 Ma based on all of the data (MSWD = 1.4). This age is consistent with the concordia age obtained from the GX 1731 acicular zircons.

The more equant, multi-faceted zircons from sample GX 1731 and zircons with similar morphology from the gneisses GX 1732 and 1737 share the same general internal compositional zoning characteristics, as revealed by CL imaging. Normal igneous oscillatory zoning is absent and most grains show broad bands of contrasting luminescence (e.g. Fig. 6b, c). Some internal zones have boundaries that suggest original

crystal faces and resorption features (Fig. 6b, c) or vague primary compositional zoning (Fig. 6c). However, for the most part the textures indicate complete internal recrystallization with weak sector (e.g. Fig. 6d) or chaotic zoning (e.g. Fig. 6e) being the most pronounced features. Sample GX 1737 also has a number of intergrown and completely recrystallized zircons (Fig. 6f). These textures are characteristic of rocks known to have been metamorphosed under granulite-facies conditions (Corfu *et al.* 2003), attesting to a high-grade metamorphic history for the Rosemarkie gneisses. Similar textures have been noted in zircons from the high-metamorphic grade gneisses from the mainland and offshore Lewisian Gneiss Complex (Corfu *et al.* 1998; Whitehouse & Bridgwater 2001; Love *et al.* 2004).

LA-MC-ICP-MS data from these complex zoned zircons are listed in Table 2 and summarized in Figure 7b. Data were obtained from the cores of the zircons, and in general only a single compositional zone was sampled. In a few instances the pit (c. 25 μm diameter) did sample across several compositional zones but there was no significant difference in isotope ratio or calculated age. Three main observations can be drawn from the data: sample GX 1732 is an Archaean gneiss; sample GX 1737 contains Archaean zircons that are distinctly younger than those in GX 1732; sample GX 1737 experienced new zircon growth or complete metamorphic resetting during the Palaeoproterozoic.

Zircon analyses from sample GX 1732 plot mainly as concordant to reversely discordant, giving ages between 2932 ± 8 Ma and 2808 ± 9 Ma. The older concordant analyses are from grains with central regions preserving vestiges of oscillatory zoning within euhedral grain outlines, surrounded by the broad banding. The younger concordant analyses are from zircons with broad sector and fir-tree zonation or from grains with roughly homogeneous and low CL. This age pattern suggests that the gneiss formed either from an igneous protolith emplaced at c. 2900 Ma with subsequent metamorphism, or at c. 2800 Ma under high-grade metamorphic conditions with c. 2900 Ma inheritance. The age of granulite-facies metamorphism certainly extended to c. 2800 Ma, by which time many of the zircons had undergone significant recrystallization.

462 The reversely discordant GX 1732 grains have similar $^{207}Pb/^{206}Pb$ ages to the
463 concordant grains, and correlate with ablations from low CL regions dominated by broad
464 sector or chaotic zoning. In contrast, the normally discordant data do not correlate with a
465 particular CL texture. These zircon data form an array consistent with the main period of
466 Pb-loss occurring between 0 Ma and 400 Ma, and do not show evidence of Proterozoic
467 Pb-loss (see Fig. 7b).
468
469 Sample GX 1737 has Archaean zircons that show the affects of significant Pb-loss or
470 new zircon growth in the Palaeoproterozoic. Unlike GX 1732, none of the Archaean
471 zircons in this rock show reverse discordance. Concordia ages range from 2781 ± 13 Ma
472 to 2719 ± 10 Ma, indicating a younger protolith age than GX 1732. The discordant,
473 largely Archaean grains fall in an array towards ~1750 Ma (Fig. 7b). A second Pb-loss
474 array is outlined by concordant to moderately discordant analyses. A regression through
475 these data (see Table 2) yields an upper intercept age of 1746 ± 31 Ma with a lower
476 intercept anchored at the GX 1734 monazite age of 398 Ma (MSWD = 2.6). An
477 unconstrained regression yields intercepts of 1740 ± 16 Ma and 233 +140/-150 Ma
478 (MSWD = 2.0). The data and CL textures are consistent with the gneiss being generated
479 from an Archaean protolith and metamorphosed under granulite- or upper amphibolite-
480 facies conditions between c. 2780 and 2720 Ma, followed by further upper amphibolite-
481 facies metamorphism during pervasive Laxfordian reworking at c. 1745 Ma.
482
483 Finally, the cores of a few rounded zircons from sample GX 1731 were analysed by
484 LA-MC-ICP-MS merely to determine the nature of inheritance in the leucogranite. Both
485 Archaean age and ca. 1700 Ma grains were observed, consistent with their derivation
486 from the adjacent Proterozoic-Archaean gneisses of the inlier.
487
488 **Implications of Dating**
489 The zircon U-Pb data from the two felsic and mafic gneisses sampled in the
490 Rosemarkie Inlier clearly show their Lewisianoid affinity. Protolith ages for GX 1732
491 range from c. 2930 Ma to 2810 Ma, with evidence of a granulite- or upper amphibolite-
492 facies metamorphic overprint at c. 2810 Ma. GX 1737 shows younger protolith ages

493 between 2780 Ma and 2720 Ma with evidence of Laxfordian recrystallisation at c. 1745
494 Ma. Friend *et al*. (2008) presented similar Archaean ages for the Borgie, Farr and Ribigill
495 Lewisianoid inliers of north Sutherland. The variability of ages shown by the Rosemarkie
496 samples is surprising given their proximity. It suggests the inlier contains structurally
497 interleaved slivers that represent different parts of the Lewisianoid basement to the
498 Moine succession. Interleaving of Moine and Lewisianoid rocks occurred prior to
499 emplacement of the leucogranites and the subsequent 'D_2' event. The planar nature of the
500 fabric and basement-cover contacts and lack of small- or medium-scale F_1 folding
501 suggests that this interleaving represents part of a 'D_1' ductile shear zone (see Harris,
502 1978).
503
504 The U-Pb TIMS zircon and monazite ages of 401 Ma and 398 Ma respectively
505 obtained from the two leucogranite samples date their emplacement as late Emsian.
506 Taking an average value of 399 Ma for leucogranite vein intrusion, and given that the
507 inlier was unconformably overlain by conglomerate and sandstones by late Eifelian times
508 at c. 393 Ma (Marshall *et al*. 2007), exhumation of the inlier and related deformation are
509 restricted to some 6 million years. Leucogranite deformation textures, metamorphic
510 assemblages in the Moine pelitic rocks, and the fabrics and fold geometries now exposed
511 are all indicative of mid-crustal levels. Hence, c. 12-15 km uplift apparently occurred in a
512 maximum time frame of 6 Ma. However, given that this period included planation of the
513 topography and generation of the overlying erosional surface, 4 to 5 million years would
514 be a more realistic estimate. Implied exhumation rates for the Rosemarkie Inlier thus
515 range from 2 mm/year to about 4 mm /year. The early Devonian Lower ORS succession
516 is present on the NW side of the GGF but absent from its immediate SE side except
517 offshore. However, outliers of Lower ORS rocks are present farther east in the Grampian
518 Highlands and there is little apparent difference in topographical level of the basal
519 unconformity across the GGF. Hence the Rosemarkie Inlier has apparently behaved as an
520 extruded, constricted, elongate 'pip' linked to sinistral transcurrent movements on the
521 GGF.
522

We now review the available structural and strain data and the regional structure to try and explain the evolution of the Rosemarkie Inlier, particularly with respect to the history of the adjacent GGF.

Structural Model

The local structure of the Learnie shore section is described above and the foliation and lineation orientations shown in Fig. 4. The foliations strike NE, orientated some 8° clockwise of the trend of the GGF, and dip moderately to steeply NW. The only measured strain values from the inlier indicate a strongly constrictional strain (Rathbone 1980) with a k value of 2.88. This obliquity of foliation, NE-plunging stretching lineation, and related D_2-D_4 prolate strain, suggest a strong component of transpression or transtension (e.g. Sanderson & Marchini, 1984; Dewey *et al*. 1998; Fossen & Tikoff, 1998). Given the proximity of the GGF and localised nature of the uplift this seems a likely circumstance. Oblate to plane strains are more generally characteristic of transpression, whereas prolate to plane strains are more typically developed in transtension (Tikoff & Teyssier 1994; Jones *et al*. 2004). Although both types of deformation can give rise to steeply dipping fabrics, they are more commonly developed in transpression. Steeply dipping lineations generally form during transpression, whereas shallow dipping, commonly horizontal lineations are typical of most transtensional situations (see Fossen & Tikoff, 1998; Krabbendam & Dewey, 1998). In the Rosemarkie Inlier the steeply dipping foliation, moderately dipping lineation (37° to 050°), and documented rapid uplift are compatible with transpression but not with transtension. The boundary conditions in effect require that the inlier is extruded, an unreasonable circumstance for a regional strain field, but plausible in small domains. It is proposed that the inlier formed at a restraining bend of the GGF due to a fault step-over to the NW that developed in mid-Devonian times. The fault geometry and the internal structure of the inlier indicate that transpressional uplift accompanied significant sinistral lateral movements on the GGF.

Theoretical transpressional deformation models and field examples on several scales have been amply documented (e.g. Robin & Cruden 1994; Lin *et al*. 1998; Jones *et al*.

554 2004). Although specific cases can be modelled, most authors have found it difficult to
555 describe the transpressional deformation fully, even in specific well-documented
556 geological examples. The variations in boundary conditions, convergence angles,
557 vorticity, strain and fabric development, strain rates, and the common occurrence of
558 strain partitioning, all impose limits on the accuracy of the model (Robin & Cruden
559 1994; Jones & Tanner 1995; Lin *et al*. 1998). In the Rosemarkie Inlier the bounding
560 faults are either unexposed or have been reactivated subsequent to mid-Devonian
561 deformation and uplift; brittle deformation effects and alteration affect much of the
562 exposed section. However, the structural geometry, strong prolate strain, and poorly
563 developed and apparently contradictory kinematic indicators seen in the Learnie shore
564 section do constrain the possible transpressional models. Tikoff & Fossen (1999)
565 provided 12 reference 3-D deformation models applicable to thrust and
566 transpressional/transtensional deformation. The Rosemarkie deformation features and
567 prolate strain fit well in the widening shear or widening/shortening shear categories,
568 dominated by vertical or possibly oblique extrusion. Robin & Cruden (1994) described
569 transpressional shear zones from Canada and Sweden and derived dynamic theoretical
570 models of the stress and strain distribution in a vertical transpression zones. Again, the
571 Rosemarkie Inlier would fit well as a sinistral transpressive zone with a strong 'Press'
572 (i.e. vertical or steep extrusion) component. One is left to speculate as to whether the
573 inlier was extruded with fixed bounding faults or became thinner as extrusion occurred.
574 Oblique transpression models introduce further complications, particularly with regard to
575 strain and vorticity variations, both across the zone and at different vertical levels (see
576 Robin & Cruden 1994, Figure 12).
577
578 Searle *et al*. (1998) documented transpressional tectonics along the dextral
579 Karakoram Fault Zone in Ladakh where a fault splay gives rise to a restraining bend. The
580 resulting inlier (the Pangong Range), which consists of Cretaceous-age migmatitic and
581 high-grade metamorphic ortho- and paragneisses (Searle *et al*. 2010), was exhumed
582 between 18 and 11 Ma. Leucogranite bodies (Tangtse Granite) were intruded at the start
583 of transpression and show S-C fabrics and a prominent lineation that plunges 20° to the
584 NW. Searle *et al*. (1998) used the offset of geological features and the lineation

585 orientation to conclude that lateral slip totalled 56 km and vertical exhumation some 20
586 km during this c. 7 Ma Miocene event, giving average lateral slip rates of 8.3 mm/year
587 and vertical uplift rates of 3.0 mm/year.
588 If we take the strain values obtained by Rathbone (1980) as representative of the
589 deformation during transpressional uplift of the Rosemarkie Inlier, then we can obtain a
590 crude estimate of the amounts of uplift and lateral movement. We must assume that:
591 i) the strongly deformed leucogranites were emplaced at the start of
592 deformation, as suggested by the field relationships
593 ii) the strain is representative of the inlier as a whole,
594 iii) the inlier is 2 km wide.
595 Approximating the inlier as a simple prolate ellipsoid and restoring it to an unstrained
596 state (Fig 8) implies uplift of c. 15 km and sinistral displacement of c. 29 km. Despite the
597 admitted simplicity of the assumptions (see above), these values are of a sensible order
598 and compatible with the structural and metamorphic state at the current level of outcrop.
599 They fit with the structural and geochronological evidence that the Rosemarkie Inlier was
600 extruded obliquely as a rising but deforming body (elongate 'pip') coeval with a short-
601 lived (4 to 6 Ma) mid-Devonian transpressional event. Lateral slip rates of 4.8 – 7.25
602 mm/year and vertical uplift rates of 2.3 – 3.65 mm/year are implied. These rates are of
603 the same order as those reported from the Yammouneh and related faults in the Lebanon
604 (Gomez *et al*. 2007; Butler *et al*. 1998), but less that those reported from major plate-
605 bounding strike-slip fault zones such as the Alpine Fault in New Zealand (Walcott, 1998)
606 or the Karakoram Fault (see above).
607 The Cromarty Inlier possibly represents a further 'pip' that was exhumed from
608 somewhat shallower crustal levels, implying that the restraining bend developed on the
609 GGF but was partitioned into blocks by linking faults, perhaps indicating that step-overs
610 developed sequentially to the northeast as sinistral movements occurred. Similarly the
611 fault-bounded sliver of Lower ORS rocks that lies adjacent to the Precambrian rocks of
612 the Rosemarkie Inlier on its southwestern side (Fig. 2.) appears to represent only limited
613 uplift during transpression.
614
615 **Discussion**

Tectonic Implications

Transpressional uplifts are a well-documented phenomenon linked to restraining bends in strike-slip fault zones. The Rosemarkie Inlier is a good small-scale example of a sharp restraining bend within a cratonic strike-slip fault system based on older crustal faults and removed from active plate boundaries. Mann (2007) provided an extensive overview and classification of restraining- and releasing bends related to active and ancient strike-slip fault systems. He noted that the bends act as 'concentrators' of intraplate stresses and the related uplifts affect relatively small rhomboidal step-over areas. Such bends are typically short-lived as they are bypassed by subsequent faulting or become extinct with continuing lateral movement. Examples of small-scale focused uplift have been reported from the San Gabriel Mountains adjacent to the San Andreas Fault (Buscher & Spotila 2007), and from the Ocotillo Badlands (8 km x 2 km step-over) along the active Coyote Fault in Southern California (Segall & Pollard, 1980). In contrast, Paul *et al*. (1999) described a c. 500 Ma example from the northern Flinders Ranges (South Australia) where localised sinistral transpressional uplift occurred during the Delamerian Orogeny. Uplift was accompanied by very high heat flows with the exhumed metamorphosed basement rock assemblages implying that temperatures of 500-550°C were attained at depths of c. 10 km.

Late Silurian – Mid-Devonian evolution of the Great Glen Fault (GGF)

As noted above the GGF has had a lengthy history of movement dominated in Silurian and Devonian times by sinistral lateral displacements. Most authors favour at least 200 kilometres of late Silurian sinistral movement based on the offset of Caledonian regional tectonic features (e.g. Dewey & Strachan, 2003) and prominent geophysical reflectors in the upper mantle lithosphere (Hall *et al*. 1984; Snyder & Flack 1990). The GGF appears to have acted as a near planar sub-vertical structure from Neoproterozoic to early Devonian times (see Stewart *et al*. 1999, 2001), but its subsequent geometry in the Moray Firth area is more complex. The Rosemarkie Inlier lacks evidence of linear or planar fabrics formed during the late Silurian sinistral movements along the GGF at c. 425 Ma. The planar fabrics that predate the leucogranite sheets and veins lie near parallel to bedding and relate to the earlier interleaving of Moine and Lewisianoid rocks. Hence,

the formation of the restraining bend, related step-overs and main structures in the inlier are mid-Devonian in age. So why did the geometry of the GGF change at this time?

Watson (1984) estimated that regional uplift of the Inverness area totalled some 10-15 km during the late Silurian-early Devonian period. The bulk of uplift was completed prior to deposition of the Lower ORS lacustrine and fluvial sandstone, siltstone and conglomerate succession that commenced in the Emsian at c.407 Ma. Thick bituminous mudstone, siltstone and impure limestone units are developed both in the Beauly-Strathpeffer area (Mykura & Owens 1983), NW of the GGF, and also beneath the Mesozoic units of the Inner Moray Firth, SE of the GGF (Marshall & Hewett 2003). These lacustrine rocks form part of the Struie Formation and attain over 1000m in thickness. The Lower ORS facies distribution and sedimentology define a pattern of restricted fault-controlled basins with proximal infill marking a period of extension (Trewin & Thirlwall 2002; Marshall & Hewett 2003). Possibly the GGF was reactivated in transtension at this time (Dewey & Strachan, 2003). During end Caledonian uplift and extension new faults were formed and the structural template was changed. Hence, when sinistral transpression occurred in the mid-Devonian as a result of a northward directed compressive 'pulse', lateral movement stepped northwest. This short-lived deformation event (399-393 Ma) signalled a marked change in the applied stress direction, apparently focused on the GGF and in the adjacent early Devonian basins where localised thrusting, folding and faulting occurred.

Late Palaeozoic – Mesozoic evolution of the Great Glen Fault (GGF)

Underhill & Brodie (1993) evaluated the structural geology of Easter Ross and the Moray Firth basin and described a sequence of NNE-trending folds and faults lying NW of the GGF trace in Middle and Upper ORS rocks around Tain. They concluded that the structures, developed during Permo-Carboniferous inversion, reflected major faults in the underlying early Devonian and older rocks. Limited dextral movements occurred on the adjacent GGF. However, the main offshore extension of the GGF was inactive during widespread extension in the Permo-Triassic and Jurassic and the fault zone was only reactivated as part of a transtensional flower structure in the late Cretaceous or early

Cainozoic. Fault movements from Jurassic times onward were focused at the margins of the Moray Firth Basin (Andrews *et al*. 1990). Bird *et al*. (1987) showed that during the Mesozoic lateral movements transferred to the northwest onto the Helmsdale Fault giving rise on the Sutherland Terrace to localised extensional deformation during sinistral movements, and inversion and localised compression during dextral movements. This migration of movement resulted in formation of a series of step-overs linked in the Mesozoic sequences by moderate to gently dipping thrusts or extensional faults. Hence, the onshore and offshore record shows that strike-slip movements migrated northwestwards onto parallel faults with their timing dependent on the regional plate tectonic geometry and the prevailing stress orientations (Underhill & Brodie, 1993). The northeast extension of the GGF into the Moray Firth Basin was locked for much of the Late Palaeozoic and Mesozoic. Underhill and Brodie (1993) concluded that because the GGF was a vertical structure and lay orthogonal to the northwest-southeast extensional strain field, strike-slip reactivation only occurred when extensional slip vectors changed to become near-parallel to the fault., i.e. in the Permo-Carboniferous and Cainozoic. Thus, the mid-Devonian transpressional event marked a major change in the pattern of movement on the GGF, with the locus of fault movement migrating progressively northwest; this pattern continued into Mesozoic times with lateral and vertical movements becoming focused on the Helmsdale Fault (Roberts & Holdsworth 1999).

The generation of the Rosemarkie Inlier

It is proposed that the Rosemarkie Inlier was generated by oblique extrusion at a sharp restraining bend developed on the GGF between about 399 Ma and 393 Ma. The formation of the step-over reflected the regional stress conditions that prevailed during this sinistral transpressional event, the increased frictional resistance to renewed movement along the pre-existing GGF trace, and the newly formed structural template. This short-lived mid-Devonian transpressional event marked the end of late Caledonian uplift, extension and sinistral transtension in the late Silurian and early Devonian (see Dewey and Strachan 2003). The event was coeval with the Acadian compressional event that is widely developed in England and Wales (Woodcock & Soper 2006; Woodcock *et al*. 2007) and even recorded in western Ireland (Meere & Mulchrone 2006). In contrast,

in West Norway and possibly also in Shetland there is evidence of widespread extension, transtension, and strike-slip fault movements during this period, which was dominated by the uplift and erosion of the emerging Caledonide chain (Krabbendam & Dewey 1998; Walsh *et al*. 2007; Fossen, 2010). Although the Acadian event resulted from the onset of collisional activity in the developing Rheic Ocean south of Avalonia we argue below that it also affected Scotland giving rise to localised sinistral transpression focused along the main terrane-bounding faults and extending as far north as the Moray Firth.

The nature of the Acadian Event in Scotland

The Devonian succession in Scotland contains evidence of periods of uplift and possible tectonic activity that separate it into three distinct sequences. These were termed the Lower, Middle and Upper Old Red Sandstone (ORS) by Murchison (1859) and the terms are still in use today, albeit with considerably modifications (see Trewin & Thirlwall 2002).

Midland Valley

The Midland Valley terrane is separated from the Highlands on its northwest side by the Highland Boundary Fault Zone (HBFZ) and from the Southern Uplands on its southeast side by the Southern Uplands Fault (SUF) (Fig. 8). Within this terrane, fluvial and lacustrine Lower ORS rocks of late Silurian to early Devonian age are widely developed (Bluck 2000). In Strathmore the sequence consists mainly of fluvial sandstones and conglomerates with volcanic rocks in its lower parts. These include the distinctive dacitic Lintrathen Tuff (Porphyry), dated at 415 ± 6 Ma (Thirlwall 1988). In its uppermost parts thick conglomerate units are developed locally adjacent to the HBFZ. A prominent example is the c.1500 m thick Strathfinella Hill Conglomerate near Fettercairn that represents a proximal alluvial fan deposit (Haughton & Bluck 1988). Unlike most conglomerate units in the Lower ORS sequence that consist largely of reworked quartzite cobbles derived from the northeast, this unit contains first cycle metamorphic and volcanic clasts, derived from the northwest. It is dominated by Dalradian psammite and semipelite clasts that can be matched readily in the nearby

740 Grampian Highlands and clearly records syn-depositional uplift of the adjacent
741 Highlands. The conglomerate passes rapidly to the southeast into siltstones and
742 mudstones which have been dated as Emsian from miospores (Richardson *et al*. 1984).
743 The Lower ORS sequence is folded into the Strathmore Syncline and Sidlaw Anticline
744 (Fig. 8) and overlapped unconformably by the late Devonian Upper ORS succession.
745 Hence fault movement, deformation, uplift, and erosion are bracketed as mid-Devonian
746 in age. The Lintrathen Tuff crops out on both sides of the HBFZ, but shows an apparent
747 sinistral offset of some 34 kilometres. The structural features and timing of deformation
748 are consistent with an Acadian sinistral transpressional event focused along the HBFZ
749 during the mid-Devonian (see Jones *et al*. 1997 for kinematic analysis; Tanner 2008).
750 Deposition of the youngest Emsian parts of the sequence appears to have overlapped with
751 fault movements along the HBFZ.
752
753 Lower ORS sandstones, conglomerates, and andesitic and basaltic volcanic rocks also
754 crop out near the southeast margin of the Midland Valley (Smith 1995) (Fig. 8). Again
755 the volcanic rocks yield a Lochkovian age, here c. 412 Ma (Thirlwall, 1988). The rocks
756 were deformed during a mid-Devonian tectonic event whose effects become more intense
757 towards the SUF. Deformation resulted in the formation of kilometre-scale, asymmetrical
758 anticlines and synclines whose axes trend NE to ENE, oblique to the SUF. They form *en*
759 *échelon* arrays and Smith (1995) interpreted the fold pattern as indicative of sinistral
760 transpression focused along the SUF. Floyd (1994) presented evidence for some 12 km
761 of sinistral offset of structures just north of the Loch Doon granite pluton.
762
763 *Meall Fuar-mhonaidh Outlier*
764 Lower ORS sandstones and conglomerates are preserved in the Meall Fuar-mhonaidh
765 outlier adjacent to the GGF some 32 km southwest of Rosemarkie (see above for details
766 of lithology and structure) (Fig. 5). The c. 2km thick sequence was deposited rapidly in a
767 fault-bounded basin (Mykura & Owens 1983). At its northeast end the Craig Nay
768 Conglomerate contains large angular clasts of psammite and pink-orange leucogranite
769 veins that match those exposed in the Rosemarkie Inlier. Given its highly proximal
770 nature and high stratigraphical position, it is proposed that this conglomerate unit formed

by erosion of the inlier, which at the time was situated immediately to the northeast. This would date the start of exhumation of the inlier and sinistral movement on the GGF as late Emsian in accord with the age of leucogranite emplacement. Note that the eroded material would be derived from a much higher crustal level than that presently exposed. The fold pattern, limited WNW-directed thrusting and decreasing strain away from the GGF in the outlier are all compatible with the development of a positive flower structure linked to sinistral transpression. Although this deformation cannot be dated with certainty here its low grade and structural pattern are best explained as due to the Acadian event.

Rosemarkie and Easter Ross

Deformation also affects the Lower ORS sequence northwest of the GGF on the Black Isle and in Easter Ross. Rogers *et al* (1989) placed the sequence in the late Emsian and noted that its northwestern bounding faults, the Torr Achilty and Glaick-Polinturk faults, show evidence of limited compressional and strike-slip reactivation. Localised thrusting occurs at the base of the succession, e.g. at Contin, and farther north on Struie Hill, where the gently ESE-dipping Struie Thrust forms a prominent feature marked by low grade mylonites (Armstrong, 1964). The thrust lies some 25 kilometres northwest of the GGF trace, and 20 km from the Cromarty Inlier (Fig.8). Underhill and Brodie (1993) deduced that the thrust formed as a consequence of footwall collapse linked to inversion along the Polinturk Fault. They interpreted the resultant flower structure as Permo-Carboniferous, linked to Variscan deformation in the Moray Firth, but its geometry is also compatible with Acadian transpression. In Easter Ross the Middle ORS sandstone and conglomerate sequence (with fish beds) overlies the Lower ORS with slight to moderate angular unconformity and is in turn overlain by Upper ORS sandstones. The whole sequence is folded by the large open Black Isle Syncline, a probable Permo-Carboniferous age structure.

The angular unconformable Middle ORS – Lower ORS boundary can be traced northeastwards into the Golspie and Badbea basins, but at Sarclet (by Wick) in Caithness the two successions are conformable (Trewin & Thirlwall, 2002), possibly documenting the northward waning of Acadian tectonic effects.

Conclusions

The Rosemarkie Inlier consists of Moine psammites and semipelites and Lewisianoid felsic and mafic gneisses, all intruded by abundant pink leucogranite veins. Zircon U-Pb LA-MC-ICP-MS data from two gneiss samples give Archaean protolith ages between 2930 and 2720 Ma; zircon morphologies are consistent with their formation in high grade gneisses at deep crustal levels. One sample contains evidence of significant zircon growth at c. 1745 Ma, indicative of Laxfordian reworking. Hence, the inlier exposes structurally interleaved Moine and Lewisianoid rocks, effectively providing a 'snapshot' of the deeper levels of the Caledonian orogen in this area. The interleaving and related planar fabrics predate leucogranite emplacement and may be late Silurian (Scandian), early Ordovician (Grampian) or Neoproterozoic (Knoydartian) in age. Similar relationships are found at the Sgurr Beag Thrust some 28 km to the WNW (Grant & Harris 2000).

Monazite and zircon U-Pb TIMS data from the leucogranite veins show that they were emplaced into the Moine and Lewisianoid rocks at 399 Ma. The veins are discordant to the early fabrics (S_1) but are strongly deformed and folded in three structural phases (D_2-D_4). Metamorphic assemblages and the structural style of the main D_2 deformation are compatible with their formation at depths of 12-15 km. The inlier is overlain unconformably by mid-Devonian (Eifelian – Givetian) sandstones and conglomerates whose deposition commenced at c. 393 Ma; thus deformation and exhumation are restricted to a maximum time frame of 6 Ma, implying local uplift rates of 2-4 mm/year.

The structure of the Rosemarkie Inlier is dominated by a generally steep NE-trending foliation (S_2), moderately NE-plunging lineation (L_2/L_3) and strongly constrictional strains (Rathbone 1980). These features are compatible with its extrusion as an elongate 'pip' at a sharp restraining bend of the Great Glen Fault (GGF) during sinistral transpression. The Rosemarkie and adjacent Cromarty inliers represent fault-bounded step-overs, formed as the locus of sinistral lateral movement on the GGF migrated onto sub-parallel faults farther to the northwest.

It is suggested that in early Devonian (Emsian) the Rosemarkie Inlier lay adjacent to the Meall Fuar-mhonaidh Outlier, now situated some 32 km to its SW. The Lower ORS sequence in the outlier contains a highly proximal conglomerate unit at its northeast end whose clasts match the lithologies of the Rosemarkie Inlier. It is proposed that the final stages of Lower ORS sedimentation in the outlier overlapped with the initial exhumation of the inlier and thus the onset of significant lateral fault movement at c. 399 Ma. The 32 km offset is broadly compatible with the strain values obtained from the deformed leucogranites and the structural geometry in the inlier.

The mid-Devonian sinistral transpressional event identified at Rosemarkie is interpreted as a manifestation of the Acadian Event, a short-lived northward-directed compressional pulse generated between 400 and 390 Ma by the collision of an Armorican microcontinent with Avalonia (Woodcock *et al*. 2007). In Scotland this pulse was focused on the main terrane-bounding fault zones, namely the Southern Upland, Highland Boundary and Great Glen fault zones. It was generally partitioned into sinistral strike-slip movements on the faults and related orthogonal compressional deformation. Intensity of deformation is greatest adjacent to the fault zones and decreases with distance away from them. Deformation was preferentially taken up by the Lower ORS sequences that had accumulated in nearby fault-bounded extensional basins. Adjacent to the HBFZ there seems to have again been an overlap of fault movement and the later phases of ORS sedimentation. Positive flower structures were formed on the northwest side of the GGF in the Meall Fuar-mhonaidh Outlier and in the Lower ORS succession in Easter Ross, e.g. the Struie Thrust. The Lower ORS – Middle ORS unconformity can be traced northwards as far as Caithness, possibly reflecting the waning effects of the Acadian Event.

The mid-Devonian (Acadian) sinistral transpression marked a significant change in the kinematics of the Great Glen Fault. Prior to this event in the late Silurian and early Devonian the fault appears to have been a planar structure and a focus for sinistral lateral movements, firstly in transpression (Stewart *et al*. 1999), but mainly in transtension

(Dewey & Strachan 2003). The end Caledonian uplift and formation of small scale basins in the early Devonian altered the structural geometry, particularly in the Moray Firth area. Hence, when the far-field Acadian effects reached northern Scotland, the GGF formed a restraining bend to facilitate the migration of lateral movement northwestwards. This pattern of fault migration was repeated in late Palaeozoic and Mesozoic times during transtensional and transpressional events, both sinistral and dextral.

Acknowledgements

The detailed mapping and observations of P.A. Rathbone in the Rosemarkie Inlier formed the basis for this study and his considerable contribution is readily acknowledged. Thanks are also due to the careful and helpful reviews by M. Stewart and N. Woodcock and some serious editing by M. Krabbendam that have resulted in a considerably more coherent and focused paper. The interpretation of the problems posed by the inlier and the history of the Great Glen Fault has benefited from discussions with A.L Harris and M. Stewart. This paper is published by permission of the Executive Director, British Geological Survey.

References

Andrews, I.J., Long, D., Richards, P.C., Thomson, A.R., Brown, S., Chesher, J.A & McCormac, M. 1990. *United Kingdom Offshore Regional Report: The Geology of the Moray Firth.* (London: HMSO for British Geological Survey)

Armstrong, M. 1964. The geology of the region between Alness River and the Dornoch Firth. *Unpublished PhD thesis, University of Newcastle upon Tyne*.

Banks, C.J. & Winchester, J.A. 2004. Sedimentary and stratigraphic affinities of Neoproterozoic coarse clastic successions, Glenshirra Group, Inverness-shire, Scotland. *Scottish Journal of Geology*, **40**, 159-174.

Bird, T.J., Bell, A., Gibbs, A.D. & Nicholson, J. 1987. Aspects of strike-slip tectonics in the Inner Moray Firth Basin, offshore Scotland. *Norsk Geologisk Tidsskrift*, **67**, 353-369.

894 Bluck, B.J. 2000. Old Red Sandstone basins and alluvial systems of Midland Scotland.
895 *In*: Friend, P.F. & Williams, B.P.J. (eds) *New Perspectives on the Old Red Sandstone*.
896 Geological Society, London, Special Publications, **180**, 417-437.
897 Buscher, J.T. & Spotila, J.A. 2007. Near-field response to transpression along the
898 southern San Andreas fault, based on exhumation of the northern San Gabriel
899 Mointains, southern California. *Tectonics*, **26**, TC5004, doi:10.1029/2006TC002017,
900 2007.
901 Butler, R.W.H., Spencer, S and Griffiths, H.M. 1998. The structural response to evolving
902 plate kinematics during transpression: evolution of the Lebanese restraining bend of
903 the Dead Sea Transform. *In*: Holdsworth, R.E., Strachan, R.A.& Dewey, J.F. (eds)
904 *Continental Transpressional and Transtensional Tectonics*. Geological Society,
905 London, Special Publications, **135**, 81-106.
906 Corfu, F., Crane, A., Moser, D. & Rogers, G. 1998. U-Pb zircon systematics at Gruinard
907 Bay, northwest Scotland: implications for the early orogenic evolution of the
908 Lewisian complex. *Contributions to Mineralogy and Petrology*, **133**, 329-345.
909 Corfu, F., Hanchar, J.M., Hoskin, P.W.O. & Kinny, P. 2003. Atlas of zircon textures.
910 *In*: Hanchar, J.M. & Hoskin, P.W.O. (eds) *Zircon: Reviews in Mineralogy &*
911 *Geochemistry*. Mineralogical Society of America and the Geochemical Society,
912 Washington DC, **53**, 469-500.
913 Corfu, F. & Noble, S.R. 1992. Genesis of the southern Abitibi greenstone belt, Superior
914 Province, Canada: Evidence from zircon Hf isotope analyses using a single filament
915 technique. *Geochimica et Cosmochimica Acta*, **56**, 2081-2097.
916 Dallmeyer, R.D., Strachan, R.A., Rogers, G., Watt, G.R. & Friend, C.R.L. 2001. Dating
917 deformation and cooling in the Caledonian thrust nappes of north Sutherland,
918 Scotland; insights from $^{40}Ar/^{39}Ar$ and Rb-Sr chronology. *Journal of Geological*
919 *Society, London*, **158**, 501-512.
920 Dewey, J.F., Holdsworth, R.E., & Strachan, R.A., 1998. Transpression and transtension
921 zones. *In*: Holdsworth, R.E., Strachan, R.A. & Dewey, J.F. (eds) *Continental*
922 *Transpressional and Transtensional Tectonics*. Special Publication of the Geological
923 Society, London, **135**, 1–14.

924 Dewey, J.F. & Strachan, R.A. 2003. Changing Silurian–Devonian relative plate motion
925 in the Caledonides: sinistral transpression to sinistral transtension. *Journal of the*
926 *Geological Society, London*, **160**, 219-229.
927 Eide, E.A., Haabesland, N.E., Osmundsen, P.T., Andersen, T.B., Roberts, D. &
928 Kendrick, M.A. 2005. Modern techniques and Old Red problems - determining the
929 age of continental sedimentary deposits with $^{40}Ar/^{39}Ar$ provenance analysis in west-
930 central Norway. *Norwegian Journal of Geology*, **85**, 133-149.
931 Fletcher, T.P., Auton, C.A., Highton, A.J., Merritt, J.W., Robertson, S. & Rollin, K.E.
932 1996. *Geology of the Fortrose and eastern Inverness District, Scotland*. Memoir of
933 the British Geological Survey, Sheet 84W (Scotland).
934 Flinn, D. 1962. On folding during three-dimensional progressive deformation. *Quarterly*
935 *Journal of the Geological Society of London*, **118**, 385-433.
936 Fossen, H. 2010. Extensional tectonics in the North Atlantic Caledonides: a regional
937 view. *In*: Law, R.D., Butler, R.W.H., Holdsworth, R.E., Krabbendam, M. & Strachan,
938 R.A. (eds) *Continental Tectonics and Mountain Building: The Legacy of Peach and*
939 *Horne*. Geological Society, London, Special Publications, **335**, 767-793.
940 Fossen, H. & Tikoff, B. 1998. Exended models of transpression and transtension, and
941 application to tectonic settings. *In*: Holdsworth, R.E., Strachan, R.A. & Dewey, J.F.
942 (eds) *Continental Transpressional and Transtensional Tectonics*. Geological Society,
943 London, Special Publications, **135**, 15-33.
944 Floyd, J.D. 1994. The derivation and definition of the 'Southern Upland Fault': a review
945 of the Midland Valley – Southern Uplands terrane boundary. *Scottish Journal of*
946 *Geology*, **30**, 51-62.
947 Freeman, S.R., Butler, R.W.H., Cliff, R.A. & Rex, D.C. 1998. Direct dating of mylonite
948 evolution: a multi-disciplinary geochronological study from the Moine thrust zone,
949 NW Scotland. *Journal of the Geological Society, London*, **155**, 745-758.
950 Friend, C.R.L., Strachan, R.A. & Kinny, P.D. 2008. U-Pb zircon dating of basement
951 iniers within the Moine Supergroup, Scottish Caledonides: implications of Archaean
952 protolith ages. *Journal of the Geological Society, London*, **165**, 807-815.
953 Gomez, F., Karam, G., Khawlie, M., McClusky, S., Vernant, P., Reilinger, R., Jaafar, R.,
954 Tabet, C., Khair, K. & Barazangi, M. 2007. Global Positioning System measurements

of strain accumulation and slip transfer through the restraining bend along the Dead Sea fault system in Lebanon. *Geophysical Journal International*, **168**, 1021-1028.

Goodenough, K.M., Evans, J.A. & Krabbendam, M. 2006. Constraining the maximum age of movements in the Moine Thrust Belt: dating the Canisp Porphyry. *Scottish Journal of Geology*, **122**, 77-81.

Gradstein, F.M., Ogg, J.G., and Smith, A.G. 2004. *A Geologic Time Scale 2004*. Cambridge University Press, Cambridge, 589 pp.

Grant, C.J. & Harris, A.L. 2000. The kinematic and metamorphic history of the Sgurr Beag Thrust, Ross-shire, NW Scotland. *Journal of Structural Geology*, **22**, 191-205.

Hall, J., Brewer, J.A., Matthews, D.H. & Warner, M. 1984. Crustal structure across the Caledonides from the WINCH seismic reflection profile: influences on the evolution of the Midland Valley of Scotland. *Transactions of the Royal Society of Edinburgh: Earth Sciences*, **75**, 97–109.

Harris, A. L. 1978. Metamorphic rocks of the Moray Firth District. *In*: Gill, G. (ed).*The Moray Firth Area Geological Studies*. Inverness Field Club. Inverness, 9-24.

Haughton, P.D.W. & Bluck, B.J. 1988. Diverse alluvial sequences from the Lower Old Red Sandstone of the Strathmore region, Scotland: Implications for the relationship between late Caledonian tectonics and sedimentation. *In*: McMillan, N.J., Embry, A.F. & Glass, D.J. (eds). *Devonian of the World.* Canadian Society of Petroleum Geologists, Memoir **14**, Vol. II, 269-293.

Horne, J. 1923. *The geology of the Lower Findhorn and Lower Strath Nairn, Scotland*. (Sheet 84 and part of 94). Memoir of the Geological Survey, Scotland.

Horstwood, M.S.A., Foster, G.L., Parrish, R.R. Noble, S.R. & Nowell G.M. 2003. Common-Pb corrected *in situ* U–Pb accessory mineral geochronology by LA-MC-ICP-MS. *Journal of Analytical Atomic Spectrometry*, **18**, 837-846.

Hutton, D.H.W. 1988. Igneous emplacement in a shear-zone termination; the biotite granite at Strontian, Scotland. *Bulletin of the Geological Society of America*, **100**, 1392-1399.

Hutton, D.H.W. & McErlean, M. 1991. Silurian and Early Devonian sinistral deformation of the Ratagain granite, Scotland: Constraints on the age of Caledonian

movements on the Great Glen fault system. *Journal of the Geological Society, London*, **148**, 1–4.

Johnson, M.R.W., Kelly, S.P., Oliver, G.J.H. & Winter, D.A. 1985. Thermal effects and timing of thrusting in the Moine thrust zone. Journal Geological Society, London, **142**, 863-874.

Johnston, S., Hacker, B.R. & Ducea, M.N. 2007. Exhumation of ultrahigh-pressure rocks beneath the Hornelen segment of the Nordfjord-Sogn Detachment Zone, western Norway. *Bulletin of the Geological Society of America*, **119**, 1232-1248.

Johnstone, G. S. & Mykura, W. 1989. *British Regional Geology: The Northern Highlands*. British Geological Survey, HMSO, Edinburgh.

Jones, R.R. & Tanner, P.W.G. 1995. Strain partitioning in transpression zones. *Journal of Structural Geology*, **17**, 793-802.

Jones, R.R., Holdsworth, R.E. & Bailey, W. 1997. Lateral extrusion in transpression zones: the importance of boundary conditions. *Journal of Structural Geology*, **19**, 1201-1217.

Jones, R.R., Holdsworth, R.E., Clegg, P., McCaffrey, K. & Tavernelli, E. 2004. Inclined transpression. *Journal of Structural Geology*, **26**, 1531-1548.

Kennedy, W.Q., 1946. The Great Glen Fault, *Quarterly Journal of the Geological Society of London*, **102**, 41–76.

Krabbendam, M. & Dewey, J.F. 1998. Exhumation of UHP rocks by transtension in the Western Gneiss Region, Scandinavian Caledonides. *In*: Holdsworth, R.E., Strachan, R.A. & Dewey, J.F. (eds) *Continental Transpressional and Transtensional Tectonics*. Geological Society, London, Special Publications, **135**, 159-181.

Krogh, T.E. 1973. A low contamination method for the hydrothermal decomposition of zircon and extraction of U and Pb for isotopic age determinations. *Geochimica et Cosmochimica Acta*, **37**, 485–494.

Krogh, T.E. 1982. Improved accuracy of U–Pb zircon ages by the creation of more concordant systems using an air abrasion technique. *Geochimica et Cosmochimica Acta* **46**, 637–649.

Leloup, P.H., Lacassin, R., Tapponier, P., Schaerer, U., Zhong Dalai, Liu Xiaohan, Zhang Liangshang, Ji Shaochemg, Phan Trong Trinh. 1995. The Ailao Shan – Red River

1016 shear zone (Yunnan, China), Tertiary transform boundary of Indochina.
1017 *Tectonophysics*, **251**, 3-84.
1018 Lin, S., Jiang, D. & Williams, P.F. 1998. Transpression (or transtension) zones of triclinic
1019 symmetry; natural example and theoretical modelling. *In*: Holdsworth, R.E., Strachan,
1020 R.A. & Dewey, J.F. (eds) *Continental Transpressional and Transtensional Tectonics*.
1021 Geological Society, London,Special Publications, **135**, 41-57.
1022 Love, G.J., Kinny, P.D. & Friend, C.R.L. 2004. Timing of magmatism and
1023 metamorphism in the Gruinard Bay area of the Lewisian Gneiss Complex:
1024 comparisons with the Assynt Terrane and implications for terrane accretion.
1025 *Contributions to Mineralogy and Petrology*, **146**, 620-636.
1026 Ludwig, K.R. 1993. PbDat: a computer program for processing Pb–U–Th isotope data,
1027 version 1.24. *US Geological Survey Open-file Report*.
1028 Ludwig, K.R. 2003. *ISOPLOT 3.00: A Geochronological Toolkit for Microsoft Excel.*
1029 Berkeley Geochronology Center, Berkeley, California.
1030 Mann, P. 2007. Global catalogue, classification and tectonic origins of restraining- and
1031 releasing bends on active and ancient strike-slip fault systems. *In*: Cunningham, W. D
1032 & Mann, P. (eds) *Tectonics of Strike-Slip Restraining and Releasing Bends*.
1033 Geological Society, London, Special Publications, **290**, 13-142.
1034 Marshall J.A.E. & Hewett, A.J. 2003. Devonian. *In*: Evans, D., Graham, C., Armour, A.
1035 and Bathurst, P., (eds) *The Millenium Atlas: Petroleum Geology of the Central and*
1036 *Northern North Sea*, Geological Society of London, London. 65–81.
1037 Marshall J.A.E., Astin, T.R., Brown, J.F., Mark-Kurik, E. & Lazauskiene, J. 2007.
1038 Recognizing the Kačák Event in the Devonian terrestrial environment and its
1039 implications for understanding land-sea interactions. *In*: Becker, R.T. & Kirchgasser,
1040 W.T. (eds) *Devonian Events and Correlations*. Geological Society, London, Special
1041 Publications, **278**, 133-155.
1042 Mattinson, J.M. 2005. Zircon U–Pb chemical abrasion ("CA-TIMS") method: Combined
1043 annealing and multi-step partial dissolution analysis for improved precision and
1044 accuracy of zircon ages. *Chemical Geology*, **220**, 47-66.

1045 Meere, P.A. & Mulchrone, K.F. 2006. Timing of deformation within Old Red Sandstone
1046 lithologies from the Dingle Peninsula, SW Ireland. *Journal of the Geological Society,*
1047 *London*, **163**, 461-469.
1048 Murchison, R.I. 1859. On the succession of the older rocks in the northernmost counties
1049 of Scotland. *Quarterly Journal of the Geological Society, London*, **15**, 353-418.
1050 Murphy, M.A., Yin, A., Kapp, P., Harrison, T.M., & Manning, C.E., 2002, Structural and
1051 thermal evolution of the Gurla Mandhata metamorphic core complex, southwest
1052 Tibet. *Geological Society of America Bulletin*, **114**, 428–447.
1053 Mykura, W. & Owens, B. 1983. The Old Red Sandstone of the Mealfuarvonie Oultier,
1054 west of Loch Ness, Inverness-shire. *Institute of Geological Sciences*, Report **83/7**.
1055 London: HMSO 17 pp.
1056 Noble, S.R. & Searle, M.P. 1995. Age of crustal melting and leucosome formation from
1057 U–Pb zircon and monazite dating in the western Himalaya, Zanskar, India. *Geology*,
1058 **23**, 1135–1138.
1059 Osmundsen, P.T. & Andersen, T.B. 2001. The middle Devonian basins of western
1060 Norway: sedimentary response to large-scale transtensional tectonics?
1061 *Tectonophysics*, **332**, 51-68.
1062 Paul, E., Flöttmann, T. & Sandiford, M. 1999. Structural geometry and controls on
1063 basement-involved deformation in the northern Flinders Ranges, Adelaide Fold Belt,
1064 South Australia. *Australian Journal of Earth Sciences*, **46**, 343–354.
1065 Rathbone, P.A. 1980. *Basement-cover relationships at Lewisian inliers in the Moine*
1066 *Series of Scotland, with particular reference to the Sgurr Beag Slide*. Unpublished
1067 PhD thesis, University of Liverpool.
1068 Rathbone, P.A. & Harris, A.L. 1980. Moine and Lewisian near the Great Glen Fault in
1069 Easter Ross. *Scottish Journal of Geology*, **16**, 51-64.
1070 Richardson, J.B., Ford, J.H. & Parker, J. 1984. Miospores, correlation and age of some
1071 Scottish Lower Old Red Sandstone sediments from the Strathmore region (Fife and
1072 Angus). *Journal of Micropalaeontology*, **3**, 109-124.
1073 Roberts, A.M. and Holdsworth, R.E. 1999. Linking onshore and offshore structures:
1074 Mesozoic extension in the Scottish Highlands. *Journal of the Geological Society,*
1075 *London*, **156**, 1061-1064.

1076 Robin, P, -Y, F. & Cruden, A.R. 1994. Strain and vorticity patterns in ideally ductile
1077 transpression zones. *Journal of Structural Geology*, **16**, 447-466.
1078 Rogers, D.A., Marshall, J.E.A. & Astin, T.R. 1989. Devonian and later movements on
1079 the Great Glen fault system, Scotland. *Journal of the Geological Society, London*,
1080 **146**, 369-372.
1081 Rogers, G. & Dunning, G. R. 1991. Geochronology of appinitic and related granitic
1082 magmatism in the W Highlands of Scotland: constraints on the timing of transcurrent
1083 fault movement. *Journal of the Geological Society, London*, **148**, 17-27.
1084 Sanderson D.J. & Marchini, W.R.D. 1984. Transpression. *Journal of Structural Geology*,
1085 **6**, 449–458.
1086 Schärer, U. 1984. The effect of initial ^{230}Th disequilibration on U-Pb ages: The Makalu
1087 case. *Earth and Planetary Science Letters*, **67**, 191–204.
1088 Searle, M.P., Weinberg, R. & Dunlap, W.J. 1998. Transpressional tectonics along the
1089 Karakoram fault zone, northern Ladakh: constraints on Tibetan extrusion. *In:*
1090 Holdsworth, R. E., Strachan, R. A. & Dewey, J. F. (eds) *Continental Transpressional*
1091 *and Transtensional Tectonics*. Geological Society, London, Special Publications,
1092 **135**, 307–326.
1093 Searle, M.P., Parrish, R.R., Thow, A.V., Noble, S.R., Phillips, R.J. & Waters, D.J. 2010.
1094 Anatomy, age and evolution of a collisional mountain belt: the Baltoro granite
1095 batholith and Karakoram MetamorphicComplex, Pakistani Karakoram. *Journal of*
1096 *the Geological Society, London*, **167**, 183-202.
1097 Segall, P. & Pollard, D. D. 1980. Mechanics of discontinuous faults. *Journal of*
1098 *Geophysical Research*, **85**, 4337-4350.
1099 Sherlock, S.C., Kelley, S.P., Zalasiewicz, J.A., Schofield, D.I., Evans, J.A., Merriman,
1100 R.J. & Kemp, S.J. 2003. Precise dating of low-temperature deformation: strain-fringe
1101 analysis by ^{40}Ar-^{39}Ar laser microprobe. *Geology*, **31**, 219-222.
1102 Smith, R.A. 1995. The Siluro-Devonian evolution of the southern Midland Valley of
1103 Scotland. *Geological Magazine*, **132**, 503-513.
1104 Snyder, D. & Flack, C.A. 1990. A Caledonian age for reflectors within the mantle
1105 lithosphere north and west of Scotland, *Tectonics*, **9**, 903–922.

1106 Soper, N.J., Strachan, R.A., Holdsworth, R.E., Gayer, R.A. & Greiling, R.O. 1992.
1107 Silurian transpression and the Silurian closure of Iapetus. *Journal of the Geological*
1108 *Society*, London, **149**, 871-880.
1109 Soper, N.J. & Woodcock, N.H. 2003. The lost Lower Old Red Sandstone of England and
1110 Wales: a record of post-Iapetan flexure or Early Devonian transtension? *Geological*
1111 *Magazine*, **140**, 627-647.
1112 Stacey, J.S & Kramers, J.D. 1975. Approximation of terrestrial lead isotope evolution by
1113 a two-stage model. *Earth and Planetary Science Letters*, **26**, 207-221.
1114 Stewart, M., Strachan, R.A. & Holdsworth, R.E. 1999. Structure and early kinematic
1115 history of the Great Glen Fault, Scotland. *Tectonics*, **18**, 326-342.
1116 Stewart, M., Strachan, R.A., Martin, M.W. & Holdsworth, R.E. 2001. Constraints on
1117 early sinistral displacements along the Great Glen Fault Zone, Scotland: structural
1118 setting, U–Pb geochronology and emplacement of the syn-tectonic Clunes tonalite.
1119 *Journal of the Geological Society*, *London*, **158**, 821–831.
1120 Tanner, P.W.G. 2008. Tectonic significance of the Highland Boundary Fault, Scotland.
1121 *Journal of the Geological Society*, *London*, **165**, 915-921.
1122 Thirlwall, M.F. 1988. Geochronology of Late Caledonian magmatism in northern
1123 Britain. *Journal of the Geological Society*, *London*, **145**, 951-967.
1124 Tikoff, B. & Teyssier, C. 1994. Strain modelling of displacement-field partitioning in
1125 transpressional orogens. *Journal of Structural Geology*, **16**, 1575–1588.
1126 Trewin, N.H. & Thirlwall, M.F. 2002. Old Red Sandstone. *In* Trewin, N. H. (ed) *The*
1127 *Geology of Scotland,* The Geological Society, London, 213-249.
1128 Underhill, J.R. 1991. Implications of Mesozoic-Recent basin development in the western
1129 Inner Moray Firth. *Journal of Marine and Petroleum Geology*, **8**, 359-369.
1130 Underhill, J.R. & Brodie, J.A. 1993. Structural geology of Easter Ross, Scotland:
1131 implications for movement on the Great Glen fault zone. *Journal of the Geological*
1132 *Society, London*, **150**, 515-527.
1133 Van Staal, C.R., Dewey, J.F., MacNiocaill, C. & McKerrow, W.S. 1998. The Cambrian
1134 - Silurian tectonic evolution of the northern Appalachians and British Caledonides:
1135 history of a complex, southwest Pacific-type segment of Iapetus. *In*: Blundell, D. J. &

Scott, A. C. (eds) *Lyell: the Past is the Key to the Present*. Geological Society, London, Special Publications, **143**, 199-242.

Van Staal, C.R. & Whalen, J.B. 2006 Magmatism during the Salinic, Acadian and Neoacadian orogenies. Geological Society of America, Abstracts with Programs, **38**, (2), p. 31

Walcott, R.I. 1998. Modes of oblique compression: late Cenozoic tectonics of the South Island of New Zealand. *Reviews of Geophysics*, **36**, 1-26.

Walsh, E.O., Hacker, B.R., Gans, P.B., Grove, M. & Gehrels, G. 2007. Protolith ages and exhumation histories of (ultra)high-pressure rocks across the Western Gneiss Region, Norway. *Bulletin of the Geological Society of America*, **119**, 289-301.

Watson, J.V. 1984. The ending of the Caledonian Orogeny. *Journal of the Geological Society*, *London*, **141**, 193-214.

Whitehouse, M.J. & Bridgwater, D. 2001. Geochronological constraints on Paleoproterozoic crustal evolution and regional correlations of the northern Outer Hebridean Lewisian complex, Scotland. *Precambrian Research*, **105**, 227-245.

Woodcock, N.H. & Soper, N.J. 2006. The Acadian Orogeny: the mid-Devonian phase that formed slate belts in England and Wales. *In* Brenchley, P.J. & Rawson, P.F. (eds) *The Geology of England and Wales*. Geological Society, London, 131-146.

Woodcock, N.H., Soper, N.J. & Strachan, R.A. 2007. A Rheic cause for the Acadian deformation in Europe. *Journal of the Geological Society, London*, **164**, 1023-1036.

Zagorevski, A., McNicoll, V J. & van Staal, C.R. 2007. Distinct Taconic, Salinic, and Acadian deformation along the Iapetus suture zone, Newfoundland Appalachians. *Canadian Journal of Earth Sciences*, **44**, 1567-1585.

Figure Captions

Fig. 1. Generalised geology of the area around Inverness showing the location of the Rosemarkie and Cromarty inliers.

Fig. 2. Geology of the Rosemarkie Inlier

Fig. 3 **(a)** Learnie foreshore showing the steeply dipping Moine psammites and Lewisianoid gneisses intruded by a prominent, near concordant, pink leucocratic microgranite vein. The hammer (38 cm long) marks the vein. Locality for GX 1731, 1732. [NH 7620 6124]. **(b)** Interference fold ($F_2 + F_3$) of thin leucogranite vein in Moine psammites and semipelites. [NH 767 617].

Fig. 4. Structural data from the Rosemarkie Inlier below Learnie Farm (lower hemisphere projection).

Fig. 5. Geological map of the Meall Fuar-mhonaidh Outlier showing its stratigraphy and structure (modified after Mykura & Owens 1983).

Fig. 6. Cathodoluminescence images. **(a)** acicular zircon (leucogranite - GX 1731) showing oscillatory zoning and high U (low CL) tip, **(b)** xenocrystic zircon (leucogranite - GX 1731) showing remnants of a now recrystallized primary zircon surrounded by a metamorphic zircon rim, **(c)** and **(d)** complex zoned zircons (gneiss - GX 1732) showing a possible primary zircon outline and embayed surface (c) and completely recrystallized internal structure (d), **(e)** and **(f)** chemically abraded complex zoned zircons; the conjoined grains both give ages of c. 1740 Ma (gneiss - GX 1737).

Fig. 7. Concordia diagrams showing: **(a)** ID-TIMS data for samples GX 1731 and 1734; light grey ellipses are GX 1731 zircons, medium grey ellipses are GX 1734 monazites. **(b)** LA-MC-ICP-MS data for samples GX 1731, 1732 and 1737. Black ellipses are GX 1731, medium grey ellipses are GX 1732, and white ellipses are GX 1737. Reference lines are 2781 – 1740 Ma and 1740 – 398 Ma.

Fig. 8. Strain modelling, see text for details.

Fig. 9. Acadian features in the British Isles. GGF – Great Glen Fault, HBF – Highland Boundary Fault, SUF – Southern Upland Fault. Ro – Rosemarkie Inlier, MF – Meall fuar-mhonaidh Outlier, SHC – Strathfinella Hill Conglomerate.

Table 1. *Zircon and monazite U-Pb ID-TIMS data for samples GX 1731, 1732*

		Concentrations †					Atomic ratios						Ages (Ma)			
Fractions *	Weight (µg)	U (ppm)	Pb (ppm)	Com-mon Pb(pg)	$^{206}Pb/^{204}Pb$ §	$^{208}Pb/^{206}Pb$ #	$^{206}Pb/^{238}U$ #	err	$^{207}Pb/^{235}U$ #	err	$^{207}Pb/^{206}Pb$ #	err	$^{206}Pb-^{238}U$	$^{207}Pb-^{235}U$	$^{207}Pb-^{206}Pb$	ρ**
GX 1731 Leucogranite [NH 7620 6124]																
1. zr, cl-pbr, 5:1, abr, 50-70 µm (13)	4.4	647.0	46.67	11.2	1042	0.1844	0.0642403	0.67	0.4829	0.80	0.05452	0.35	401.4	400.1	392.5	0.90
2. zr, pbr, 4:1, abr, 80-100 µm (2)	7.7	724.0	49.48	16.4	1351	0.1636	0.06315	0.34	0.4827	0.53	0.05544	0.39	394.8	399.9	429.9	0.67
GX 1734 Leucogranite [NH 7641 6144]																
3. mo, 2:1 eu, 80 µm (1)	1.0	1325	1286	5.3	1026	16.24	0.06417	0.52	0.4778	0.56	0.05401	0.21	400.9	396.6	371.4	0.93
4. mo, 2:1, eu, 90 µm (1)	1.3	935.0	977.0	7.4	683.3	17.5	0.06434	0.56	0.4783	0.66	0.05392	0.33	401.9	396.9	367.7	0.87
5. mo, 2:1, sub, 80 µm (1)	1.0	870.0	690.0	5.9	623.6	12.86	0.06492	0.77	0.4835	0.82	0.05401	0.29	405.5	400.5	371.5	0.93
6. mo, 1:1 eu, 70 µm (1)	1.2	850.0	1157	4.7	903.9	23.23	0.06410	0.35	0.4795	0.48	0.05425	0.33	400.5	397.7	381.3	0.74

* mo = monazite, zr = zircon; l:w aspect ratio; abr = air abraded; eu = euhedral, sub = subhedral; cl = colourless, pbr = pale brown; length (µm); (x) = number of grains analyzed.

† Maximum errors are ± 20%. Weights were measured on a Cahn C32 microbalance or calculated from grain dimensions measured on binocular microscope photos.

§ Measured ratio corrected for mass fractionation and common Pb in the $^{205}Pb/^{235}U$ spike.

\# Corrected for mass fractionation, spike, laboratory blank Pb and U, and initial common Pb (Stacey and Kramers 1975; calculated at 400 Ma).
The laboratory blank Pb composition is $^{206}Pb/^{204}Pb$:$^{207}Pb/^{204}Pb$:$^{208}Pb/^{204}Pb$ = 17.46: 15.55: 37.32. Quoted errors are 2 σ (% for atomic ratios, absolute for ages).

** $^{207}Pb/^{235}U$ - $^{206}Pb/^{238}U$ error correlation coefficient calculated following Ludwig (1993).

Table 2. *Zircon U-Pb LA-MC-ICP-MS data for samples GX1731, 1732, 1737*

	Concentrations †		Atomic ratios #							Ages‡ (Ma)							
Analysis	U (ppm)	Pb (ppm)	$^{206}Pb/^{238}U$	err	$^{207}Pb/^{235}U$	err	$^{207}Pb/^{206}Pb$	err	ρ**	$^{206}Pb/^{238}U$	err	$^{207}Pb/^{235}U$	err	$^{207}Pb/^{206}Pb$	err	Conc. age	Err (MSWD)
GX 1731 Leucogranite [NH 7620 6124]																	
1731-1	664	179	0.3030	0.8	4.425	0.8	0.1059	0.1	0.99	1717	24	1706	13	1730	3		
1731-2	365	108	0.3234	0.7	4.747	0.7	0.1064	0.1	0.98	1776	21	1807	12	1739	5		
1731-3	295	127	0.4725	0.8	11.46	0.9	0.1759	0.4	0.91	2562	33	2495	16	2615	12		
1731-4	267	108	0.4552	0.9	10.91	1.0	0.1738	0.4	0.92	2515	35	2418	18	2595	12		
1731-5	150	63.4	0.4490	0.9	11.02	0.9	0.1780	0.2	0.99	2525	35	2391	17	2635	5		
1731-6	80.8	33.4	0.4486	1.4	10.99	1.4	0.1777	0.3	0.98	2523	55	2389	26	2632	9		
GX 1732 Hornblende-biotite felsic gneiss [NH 7620 6124]																	
1732-1	17.8	9.6	0.5603	0.9	15.68	1.1	0.2030	0.7	0.81	2858	43	2868	21	2851	22	2854	20 (0.5)
1732-2	31.7	16.7	0.5610	0.9	15.90	1.0	0.2056	0.4	0.90	2871	40	2871	18	2871	14	2871	14 (<0.1)
1732-3	18.6	7.8	0.4390	0.8	12.05	1.1	0.1991	0.8	0.73	2608	31	2346	20	2819	25		
1732-4	61.5	31.8	0.5498	0.9	15.63	1.0	0.2062	0.2	0.97	2855	42	2824	18	2876	7		
1732-5	51.6	26.7	0.5536	0.9	15.64	1.0	0.2049	0.3	0.96	2855	42	2840	18	2866	9	2864	11 (0.5)
1732-6	13.2	6.3	0.5161	1.0	14.51	1.3	0.2039	0.9	0.74	2784	43	2683	25	2858	29		
1732-7	9.3	4.5	0.5225	1.0	13.92	1.6	0.1932	1.2	0.63	2744	45	2710	30	2770	41		
1732-8	37.7	18.7	0.5413	0.8	15.02	0.9	0.2013	0.4	0.91	2817	36	2789	17	2836	12		
1732-9	28.9	15.1	0.5533	0.8	15.46	1.0	0.2026	0.5	0.87	2844	38	2839	18	2847	15	2837	16 (1.2)
1732-10	26.8	14.3	0.5701	0.9	16.70	1.0	0.2125	0.4	0.89	2918	40	2908	18	2925	14	2923	15 (0.6)
1732-11	22.4	11.8	0.5487	0.8	15.28	0.9	0.2019	0.5	0.83	2833	35	2820	18	2842	17	2831	13 (5.9)
1732-12	61.1	32.5	0.5615	0.7	16.02	0.7	0.2070	0.2	0.95	2878	33	2873	14	2882	8	2881	10 (0.3)
1732-13	16.5	7.9	0.5087	0.8	14.09	1.1	0.2008	0.7	0.75	2756	36	2651	21	2833	24		
1732-14	76.4	40.5	0.5492	0.9	15.92	0.9	0.2102	0.2	0.98	2872	40	2822	17	2907	6		
1732-15	29.0	14.6	0.5329	0.8	14.78	0.9	0.2012	0.4	0.88	2801	37	2753	18	2836	14		
1732-16	45.6	24.1	0.5666	0.8	15.78	0.9	0.2020	0.3	0.94	2864	37	2894	16	2842	9		
1732-17	13.5	7.2	0.5754	0.9	15.78	1.3	0.1989	0.8	0.76	2864	44	2930	24	2817	27		
1732-18	125	64.1	0.5596	0.8	15.80	0.8	0.2047	0.2	0.98	2865	38	2865	16	2864	5	2864	8.3 (<0.1)
1732-19	75.6	35.3	0.5166	1.5	14.06	1.5	0.1974	0.2	0.99	2754	64	2685	28	2805	7		
1732-20	43.7	20.9	0.5251	1.1	14.13	1.2	0.1951	0.4	0.95	2758	50	2721	22	2786	12		
1732-21	72.5	33.5	0.4974	0.9	13.46	0.9	0.1963	0.2	0.96	2713	37	2603	17	2796	8		
1732-22	103	54.6	0.5789	1.0	17.04	1.0	0.2135	0.2	0.99	2937	48	2944	20	2932	5	2933	7.1 (0.9)
1732-23	109	52.4	0.5415	1.0	14.78	1.0	0.1980	0.2	0.99	2801	47	2790	20	2809	6	2809	8.7 (0.7)
1732-24	55.2	29.3	0.5590	1.1	15.85	1.2	0.2056	0.2	0.98	2868	53	2863	22	2871	8	2871	12 (0.1)
1732-25	40.3	20.3	0.5507	0.9	15.27	1.0	0.2012	0.3	0.94	2832	42	2828	19	2836	11		
1732-26	30.1	16.4	0.5863	0.8	16.75	0.9	0.2073	0.4	0.89	2921	38	2974	17	2884	13		
1732-27	86.3	43.8	0.5634	1.1	15.34	1.1	0.1975	0.3	0.96	2837	49	2881	21	2806	10		
1732-28	31.1	16.8	0.5923	0.8	16.87	0.9	0.2066	0.4	0.90	2927	39	2999	17	2879	13		
1732-29	20.5	10.7	0.5701	0.9	15.85	1.1	0.2016	0.6	0.85	2868	42	2908	20	2839	18		
1732-30	42.2	21.3	0.5521	0.8	15.50	0.8	0.2036	0.3	0.92	2846	34	2834	15	2855	10	2852	12 (1.3)
1732-31	95.3	40.4	0.4585	1.0	12.45	1.0	0.1969	0.2	0.98	2639	39	2433	18	2801	7		
1732-32	22.1	9.0	0.4440	1.3	11.89	1.5	0.1942	0.7	0.88	2596	52	2369	27	2778	23		
1732-33	103	50.9	0.5400	1.1	14.84	1.2	0.1993	0.2	0.99	2805	51	2783	22	2820	6	2819	8.8 (0.16)
1732-34	130	63.2	0.5093	1.1	13.86	1.1	0.1974	0.2	0.99	2740	48	2654	21	2805	5		
GX 1737 Hornblende-biotite felsic gneiss [NH 7649 6155]																	
1737-1	83.5	33.9	0.4345	1.2	10.71	1.3	0.1788	0.5	0.92	2499	47	2326	24	2642	17		

1737-2	85.2	31.3	0.3998	1.2	8.007	1.4	0.1453	0.7	0.89	2232	46	2168	25	2291	22		
1737-3	272	104	0.4183	1.1	9.533	1.1	0.1653	0.2	0.98	2391	42	2253	20	2511	8		
1737-4	349	159	0.4947	1.2	12.81	1.2	0.1878	0.1	0.99	2666	50	2591	22	2723	5		
1737-5	168	43.9	0.2882	1.2	4.153	1.3	0.1045	0.6	0.87	1665	33	1632	22	1706	24		
1737-6	353	102	0.3183	1.1	5.275	1.1	0.1202	0.4	0.94	1865	34	1782	19	1959	13		
1737-7	478	214	0.4893	1.1	12.00	1.1	0.1779	0.1	0.99	2605	47	2568	21	2634	4		
1737-8	362	163	0.5029	1.1	13.09	1.1	0.1887	0.2	0.99	2686	47	2626	21	2731	6		
1737-9	196	73.0	0.4088	1.1	9.138	1.1	0.1621	0.3	0.95	2352	40	2209	20	2478	12		
1737-10	264	93.2	0.3907	1.2	9.154	1.3	0.1699	0.4	0.95	2354	43	2126	23	2557	13		
1737-11	84.7	33.9	0.4339	1.2	10.67	1.3	0.1784	0.6	0.89	2495	46	2323	24	2638	20		
1737-12	147	50.7	0.3809	1.8	8.014	1.9	0.1526	0.5	0.97	2233	64	2080	33	2375	16		
1737-15	315	140	0.4943	1.2	12.46	1.3	0.1828	0.3	0.97	2640	52	2589	24	2678	11		
1737-16	119	48.3	0.4479	1.2	10.40	1.3	0.1684	0.4	0.95	2471	48	2386	23	2542	13		
1737-17	127	51.1	0.4328	1.2	10.01	1.3	0.1677	0.5	0.93	2435	47	2318	24	2534	16		
1737-18	223	104	0.5042	1.1	13.45	1.1	0.1935	0.2	0.98	2712	47	2632	21	2772	7		
1737-19	216	82.2	0.4161	1.1	9.086	1.2	0.1584	0.4	0.95	2347	42	2243	21	2438	12		
1737-20	118	35.8	0.3344	1.2	6.711	1.3	0.1455	0.6	0.89	2074	38	1860	23	2294	21		
1737-21	234	91.1	0.4437	1.3	10.92	1.3	0.1785	0.3	0.97	2516	50	2367	24	2639	10		
1737-22	125	47.1	0.4299	1.3	10.24	1.5	0.1728	0.7	0.87	2457	50	2305	27	2585	24		
1737-23	302	84.1	0.3072	1.3	4.604	1.4	0.1087	0.5	0.93	1750	38	1727	22	1778	19		
1737-24	63.7	31.0	0.5304	1.2	13.92	1.3	0.1903	0.5	0.92	2744	54	2743	25	2745	17	2745	17 (<0.1)
1737-25	108	47.1	0.4741	1.2	11.32	1.3	0.1732	0.4	0.94	2550	49	2502	23	2588	14		
1737-26	99.8	49.0	0.5397	1.1	14.48	1.2	0.1945	0.4	0.95	2781	51	2782	22	2781	12	2781	13 (<0.1)
1737-27	152	62.3	0.4467	1.3	11.18	1.3	0.1815	0.3	0.97	2538	50	2380	24	2667	11		
1737-28	199	95.9	0.5256	1.3	13.58	1.3	0.1874	0.2	0.98	2721	57	2723	25	2719	8	2719	10 (<0.1)
1737-29	449	218	0.5163	1.3	13.81	1.3	0.1939	0.1	0.99	2736	56	2684	24	2776	4		
1737-30	255	126	0.5309	1.1	13.84	1.1	0.1892	0.2	0.99	2739	50	2745	21	2735	6	2735	9 (0.16)
1737-31	97.6	41.6	0.4535	1.2	11.29	1.3	0.1806	0.4	0.94	2547	50	2411	24	2658	15		
1737-32	109	46.7	0.4621	1.1	11.50	1.2	0.1804	0.4	0.94	2564	45	2449	22	2657	14		
1737-33	281	101	0.3832	1.2	8.997	1.3	0.1703	0.3	0.98	2338	44	2091	23	2561	9		
1737-34	168	72.8	0.4636	1.2	11.43	1.3	0.1788	0.4	0.95	2559	51	2456	24	2641	14		
1737-35	44.5	13.8	0.3296	1.2	5.123	2.0	0.1127	1.6	0.58	1840	37	1837	33	1844	59		
1737-36	107	49.0	0.4852	1.2	12.37	1.3	0.1849	0.4	0.95	2633	51	2550	24	2697	14		
1737-37	216	38.2	0.1901	1.2	2.710	1.9	0.1034	1.5	0.62	1331	25	1122	28	1686	56		
1737-38	110	33.3	0.3244	1.3	4.839	1.5	0.1082	0.8	0.86	1792	41	1811	25	1769	28		
1737-39	101	30.2	0.3185	1.1	4.731	1.4	0.1077	0.8	0.80	1773	35	1782	23	1761	31		
1737-40	68.0	32.3	0.5075	1.2	12.91	1.3	0.1846	0.5	0.91	2673	50	2646	24	2694	17		
1737-41	201	93.9	0.4990	1.2	12.49	1.2	0.1815	0.2	0.98	2642	51	2610	22	2666	8		
1737-42	118	33.0	0.3060	1.2	4.467	1.5	0.1059	0.8	0.84	1725	37	1721	24	1730	29		

† Errors are c. ± 10%. # Measured ratios not corrected for common Pb. ** $^{207}Pb/^{235}U$ - $^{206}Pb/^{238}U$ error correlation coefficient calculated following Ludwig (1993).

‡ Age errors quoted at the 1σ level. Concordia ages and goodness of fit expressed as MSWD were calculated using Ludwig 2003.

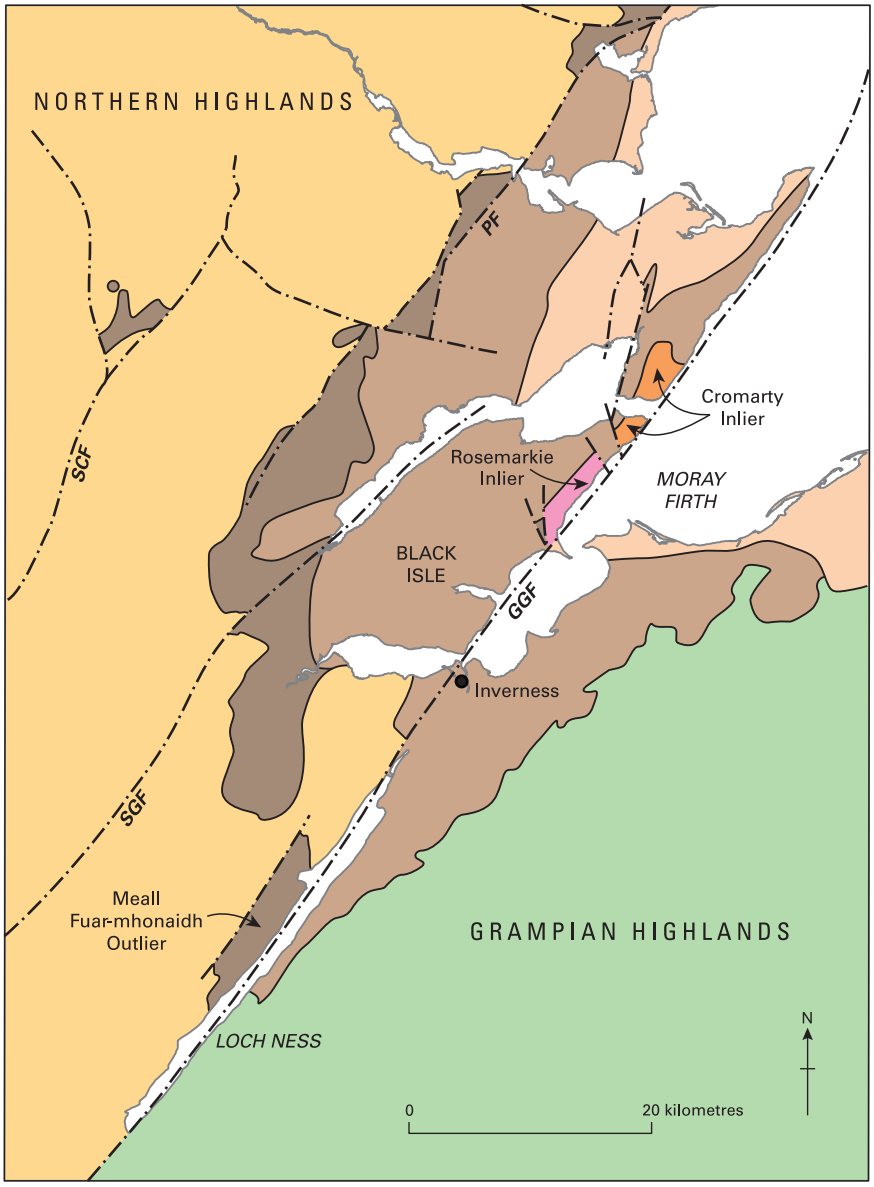

Late Devonian

Mid-Devonian

Early Devonian

Cromarty Inlier

Rosemarkie Inlier

Moine Supergroup and Neoproterozoic and Early Palaeozoic plutonic rocks

Dalradian Supergroup, older Dava and Glen Banchor successions, and Early Palaeozoic plutonic rocks

Fault

Abbreviations:
GGF - Great Glen Fault, ***PF*** - Polinturk Fault, ***SGF*** - Strath Glass Fault, ***SCF*** - Strathconon Fault
MF - Meall Fuar-mhonaidh Outlier

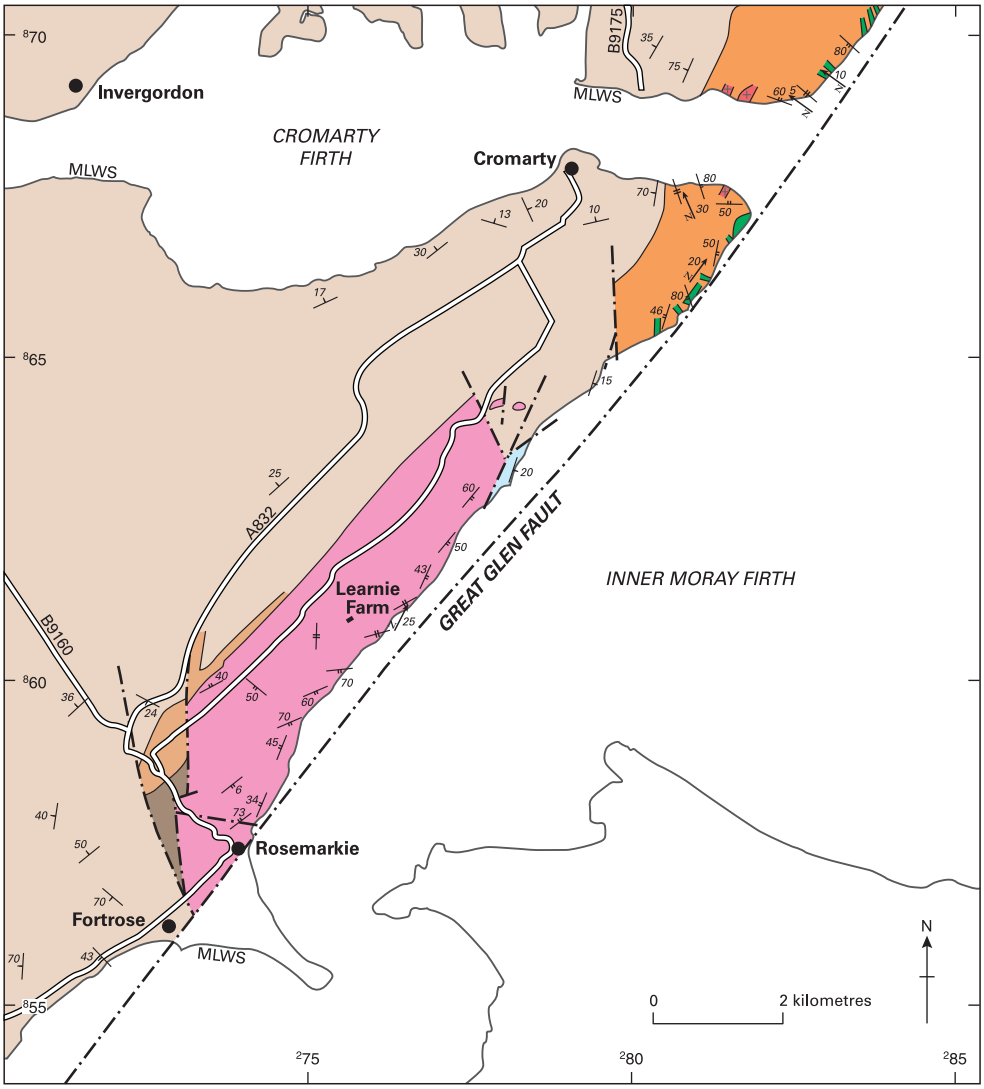

Jurassic

Shaly mudstone and sandstone

Mid-Devonian

Sandstone, minor siltstone and conglomerate lenses

Conglomerate

Early Devonian

Siltstone and micaceous sandstone, basal breccio-conglomerate

Intrusive rocks

Granite, typically pegmatitic

Mafic intrusions, typically amphibolites

Moine and Lewisianoid rocks

Cromarty Inlier - psammite and semipelite with granitic veins and pegmatitic granite patches

Rosemarkie Inlier - gneissose psammite and minor semipelite interleaved with thin-banded felsic and mafic orthogneisses; minor amphibolitic mafic pods. Leucogranite veins.

Inclined bedding, dip in degrees

Inclined foliation, dip in degrees

Vertical foliation

Axis of minor fold, plunge in degrees

Fault

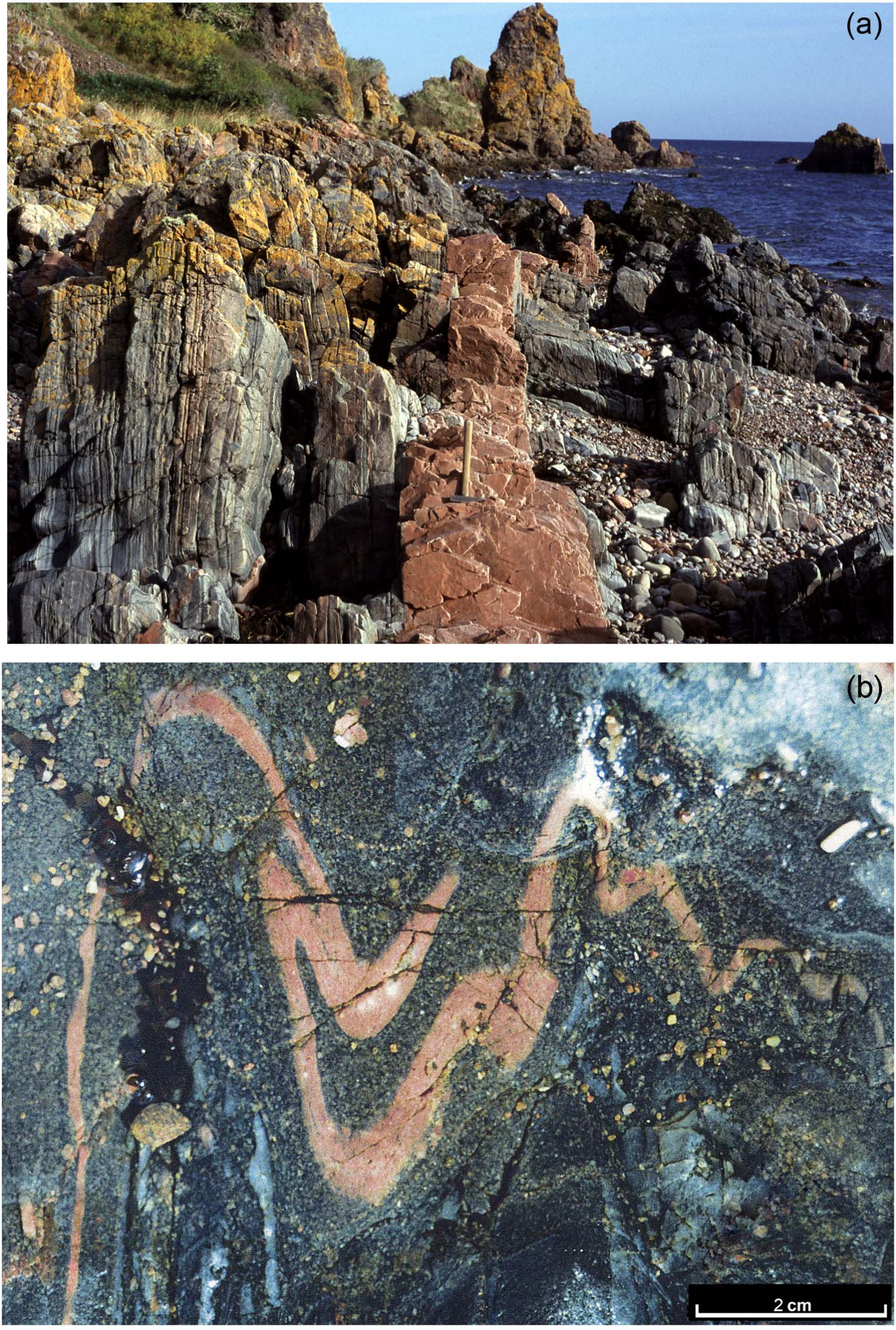
(a)
(b)
2 cm

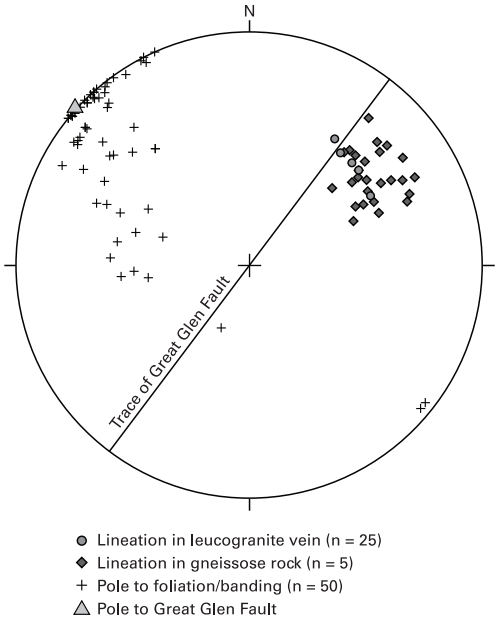
N
Trace of Great Glen Fault
Lineation in leucogranite vein (n = 25)
Lineation in gneissose rock (n = 5)
Pole to foliation/banding (n = 50)
Pole to Great Glen Fault

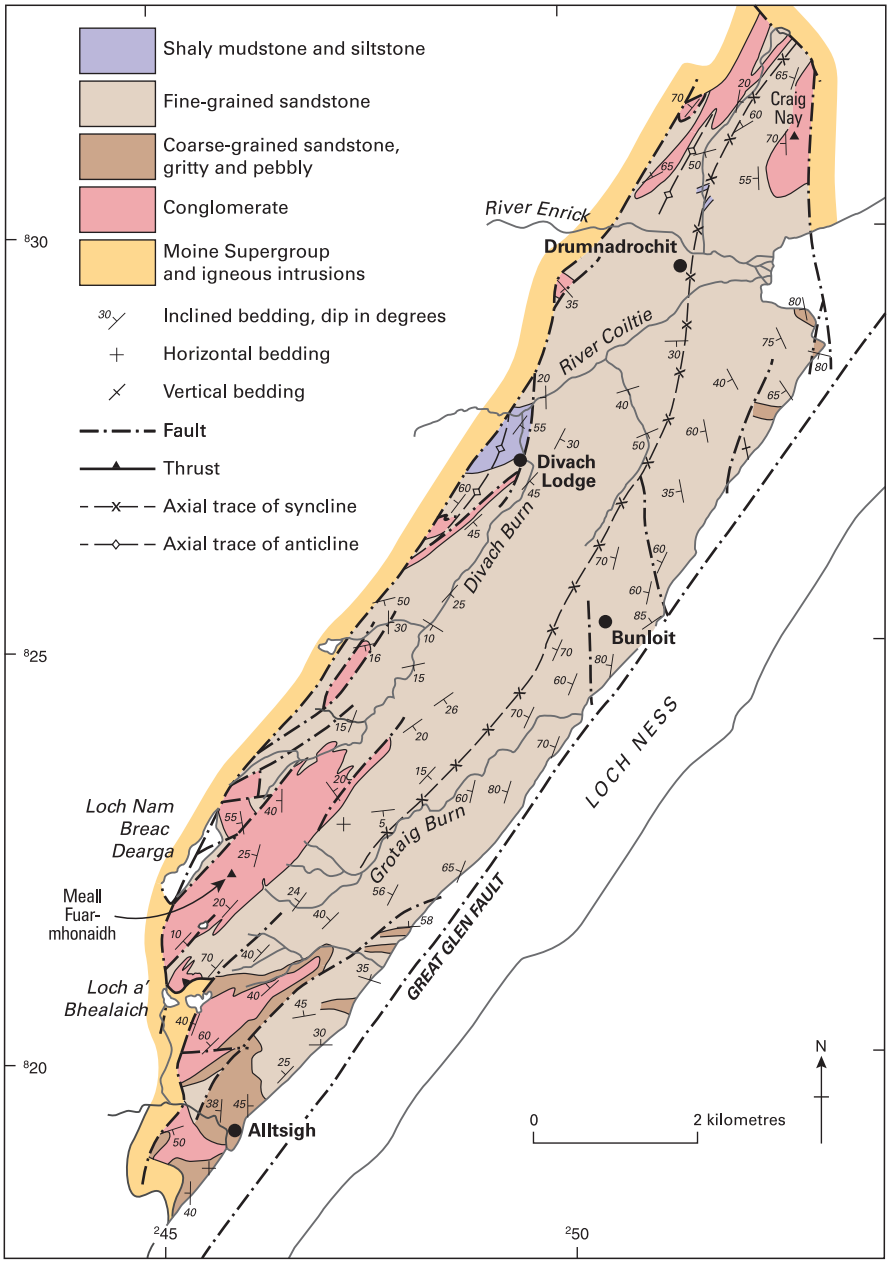
Shaly mudstone and siltstone
Fine-grained sandstone
Coarse-grained sandstone, gritty and pebbly
Conglomerate
Moine Supergroup and igneous intrusions
Inclined bedding, dip in degrees
Horizontal bedding
Vertical bedding
Fault
Thrust
Axial trace of syncline
Axial trace of anticline
Craig Nay
River Enrick
Drumnadrochit
River Coiltie
Divach Lodge
Divach Burn
Bunloit
LOCH NESS
Grotaig Burn
Loch Nam Breac Dearga
Meall Fuar-mhonaidh
Loch a' Bhealaich
GREAT GLEN FAULT
Alltsigh
N
0
2 kilometres
830
825
820
245
250

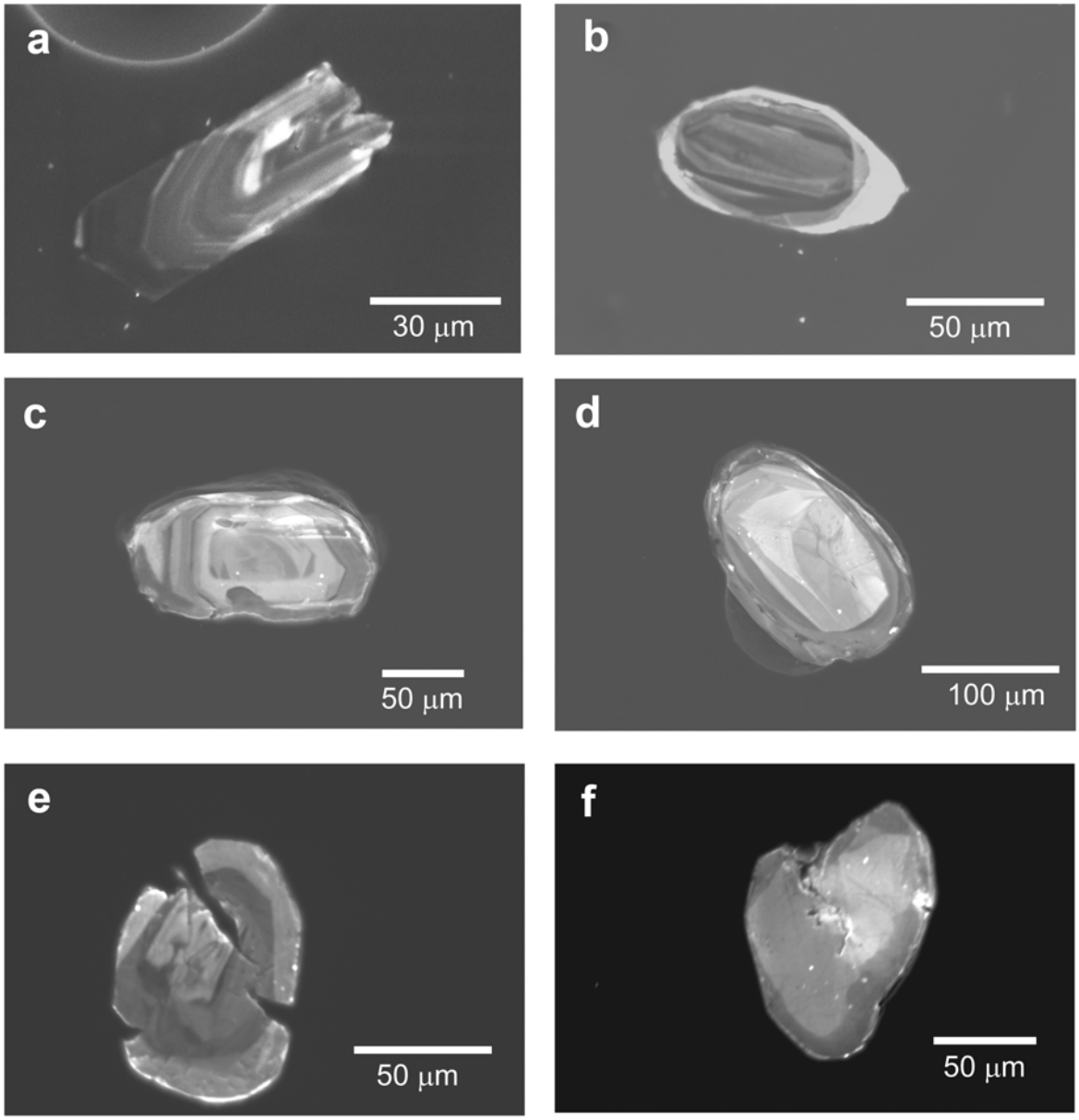
a
30 μm
b
50 μm
c
50 μm
d
100 μm
e
50 μm
f
50 μm

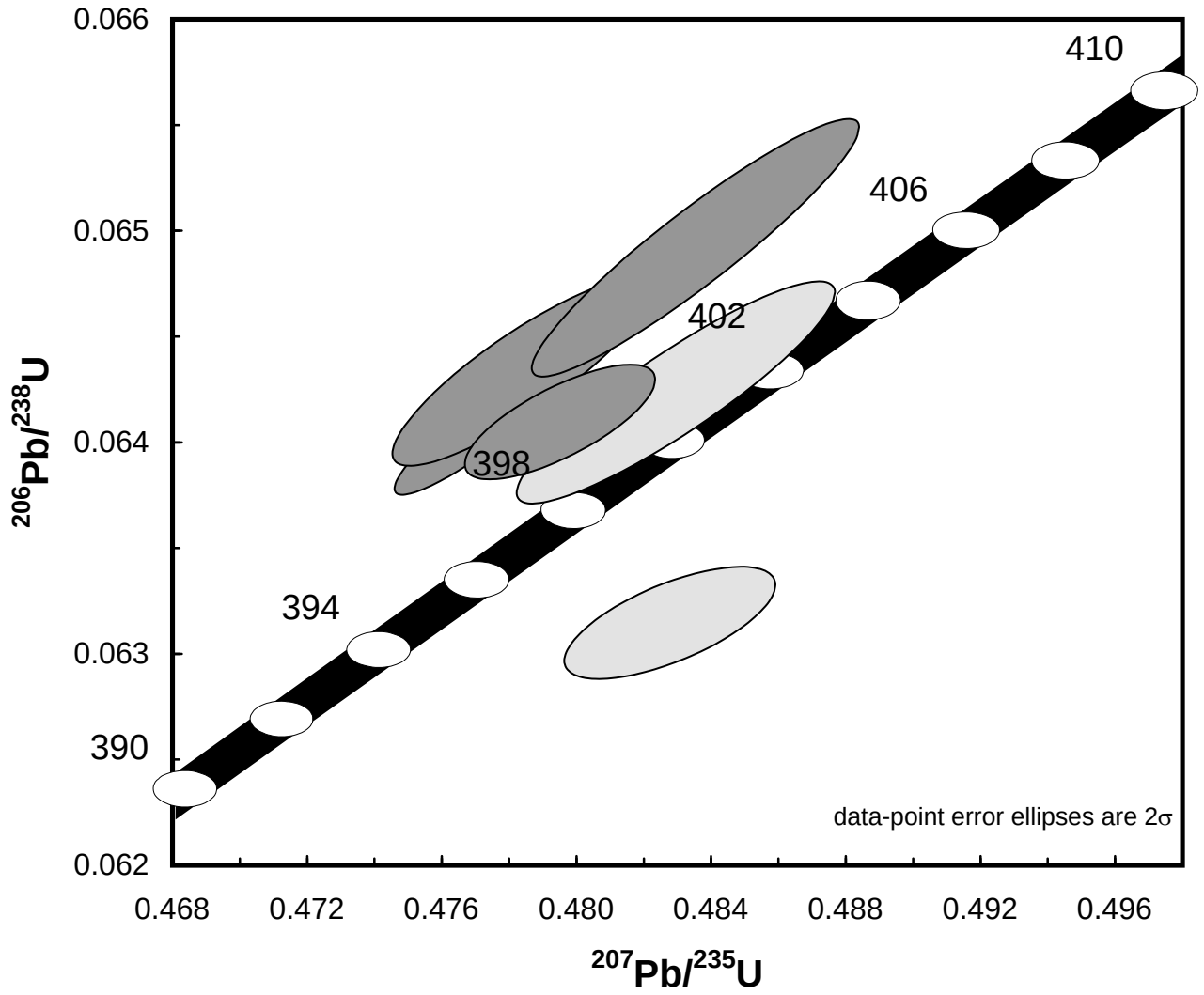
0.066
0.065
0.064
0.063
390
0.062
410
406
402
398
394
data-point error ellipses are 2σ
0.468
0.472
0.476
0.480
0.484
0.488
0.492
0.496
$^{206}Pb/^{238}U$
$^{207}Pb/^{235}U$

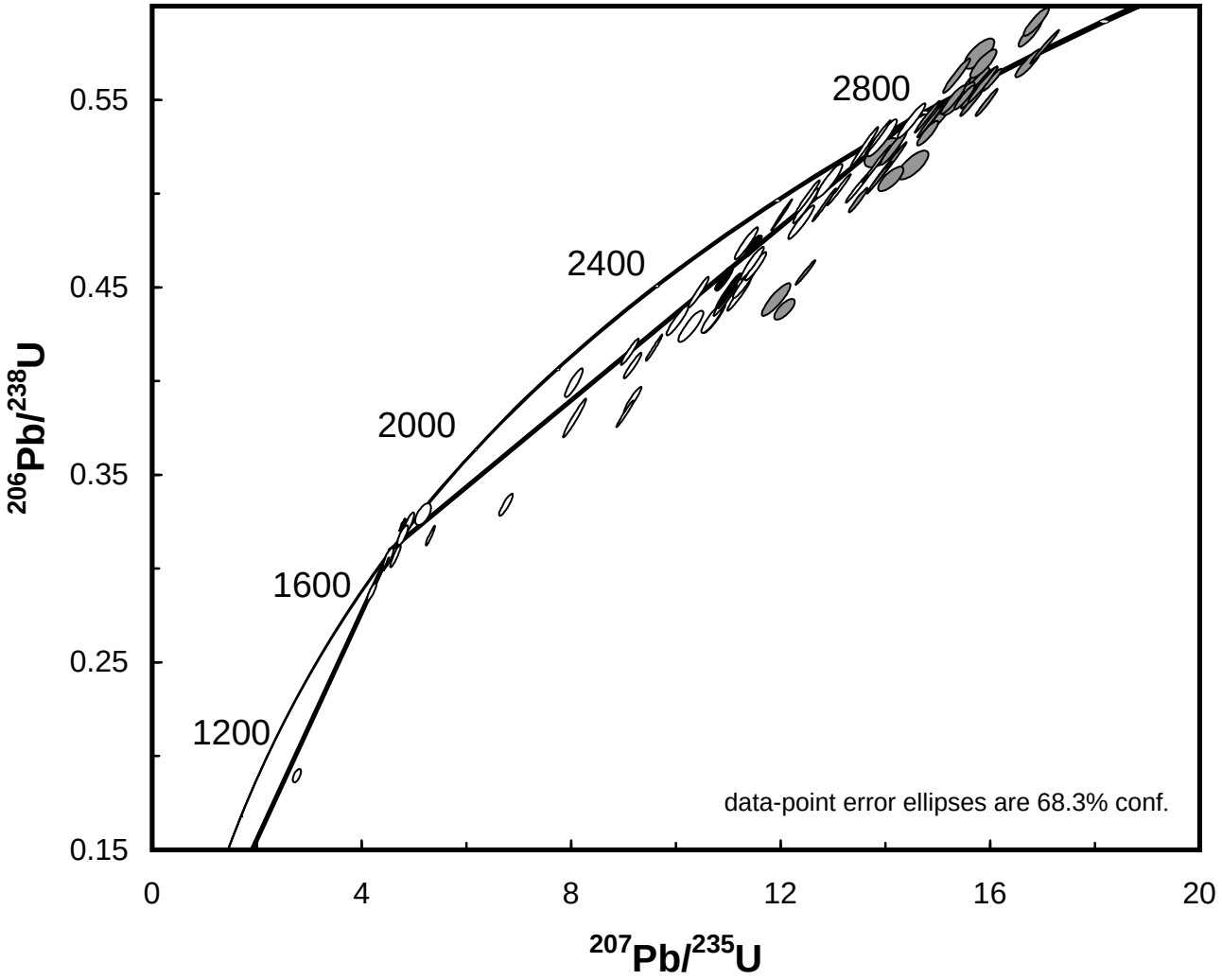
0.55
0.45
0.35
0.25
0.15
0
4
8
12
16
20
2800
2400
2000
1600
1200
data-point error ellipses are 68.3% conf.
206Pb/238U
207Pb/235U

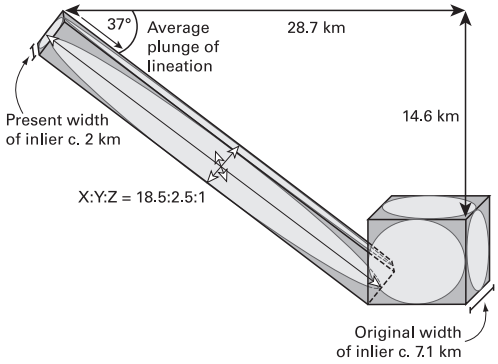
37°
Average
plunge of
lineation
28.7 km
14.6 km
Present width
of inlier c. 2 km
X:Y:Z = 18.5:2.5:1
Original width
of inlier c. 7.1 km

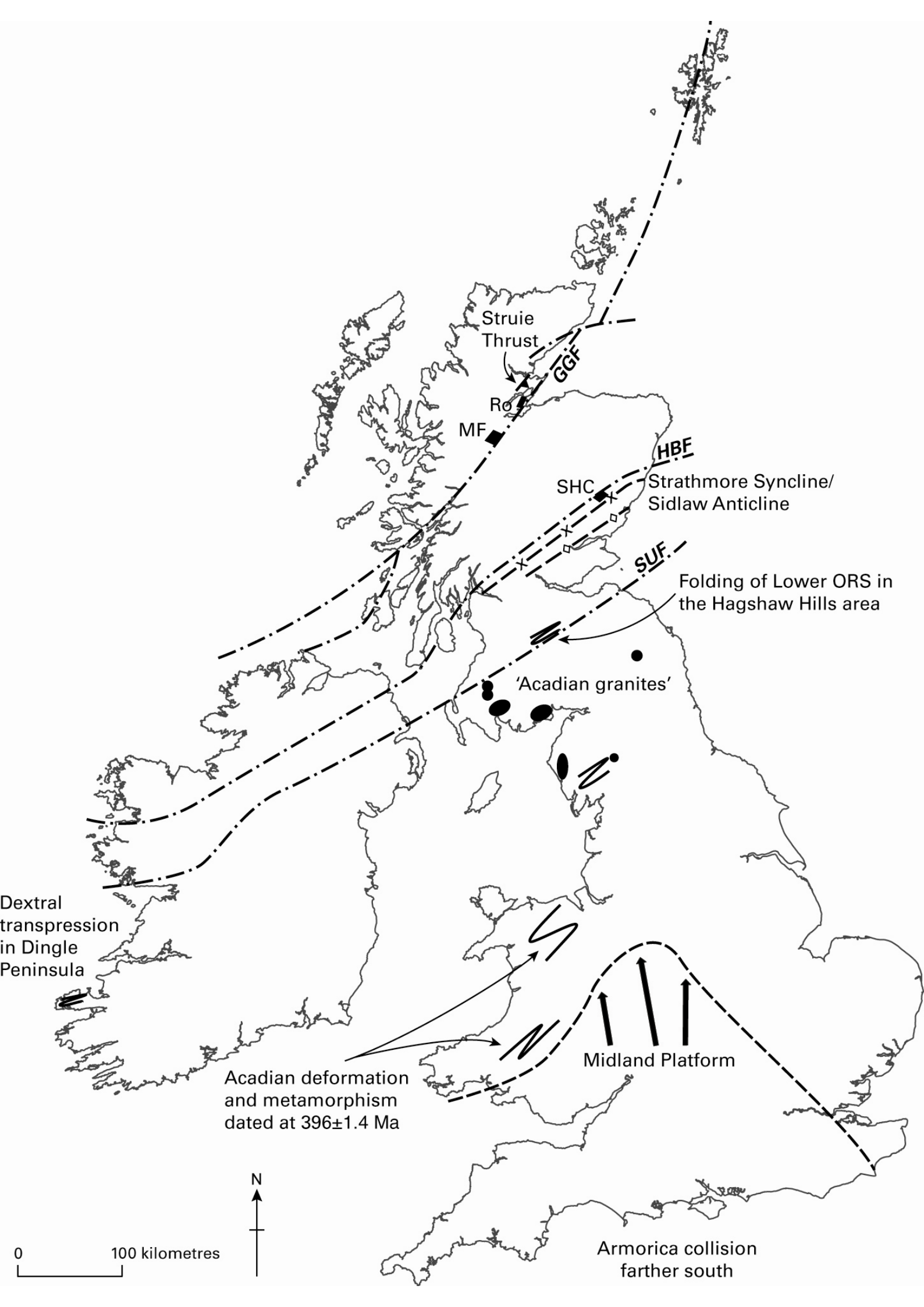
Struie
Thrust
GGF
Ro
MF
HBF
SHC
Strathmore Syncline/
Sidlaw Anticline
SUF
Folding of Lower ORS in
the Hagshaw Hills area
'Acadian granites'
Dextral
transpression
in Dingle
Peninsula
Midland Platform
Acadian deformation
and metamorphism
dated at 396±1.4 Ma
Armorica collision
farther south
N
0
100 kilometres